Available online at www.sciencedirect.com
SCIENCE DIRECT®
Coordination Chemistry Reviews 241 (2003) 249–272
COORDINATION CHEMISTRY REVIEWS
www.elsevier.com/locate/ccr

Lanthanides and actinides: annual survey of their organometallic chemistry covering the year 1997

Ji-Young Hyeon, Frank T. Edelmann *

Chemisches Institut der Otto-von-Guericke-Universität Magdeburg, Universitaetsplatz 2, D-39106 Magdeburg, Germany

Received 3 October 2002; accepted 7 October 2002

Contents

Keywords: Lanthanides; Actinides; Cyclopentadienyl complexes; Cyclooctatetraenyl complexes; Organometallic chemistry

1. Introduction

The review presents complexes of the lanthanides, actinides and also scandium and yttrium, which contain metal–carbon bonds as defined by Section 29 of Chemical Abstracts. Abstracts of papers presented at conferences, dissertations, highlights and patents have mostly been excluded.

* Corresponding author. Fax: +49-391-671-2933
E-mail address: frank.edelmann@vst.uni-magdeburg.de (F.T. Edelmann).

2. Lanthanides

2.1. Lanthanide complexes without supporting cyclopentadienyl and cyclopentadienyl-like ligands

Groth and coworkers [1] published the synthesis of new alkoxy- and amido cerium compounds of the general type $Ce(OR)_3$, $ClCe(OR)_2$ and $Ce(NR_2)_3$. The new alkoxy cerium compounds were synthesized by ligand exchange reaction. As starting material cerium tris(isopropoxide) was used (Scheme 1).

PII: S0010-8545(02)00291-6

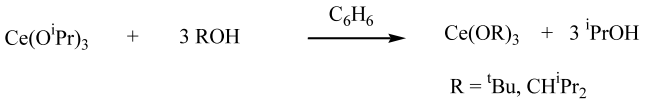

Scheme 1. Formation of alkoxy- and amido cerium compounds.

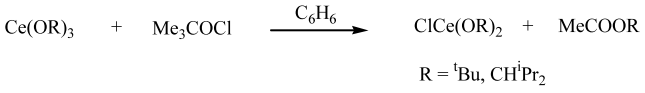

Scheme 2. Formation of chloro ceriumdialkoxides.

Scheme 3. Formation of amido cerium compounds.

The new cerium tris(alkoxide) compounds were reacted with equimolar amounts of acetyl chloride to afford chloro dialkoxycerium species (Scheme 2).

The amido cerium compounds were available by salt elimination reaction between $CeCl_3 \cdot THF$ and lithium amides (Scheme 3).

The results of enantioselective addition reactions using these cerium intermediates are presented in Section 2.6.

2.2. Complexes with cyclopentadienyl ligands

2.2.1. Mono(cyclopentadienyl) complexes

Hou et al. [2] published the synthesis and characterization of novel heteroleptic samarium(II) complexes bearing both aryloxide and pentamethylcyclopentadienyl ligands. Reactions of $(C_5Me_5)_2Sm(THF)_2$ with 1 equiv. of ArOH (Ar = $C_6H_2^tBu_2$–2,6-R-4, R = H, Me, ^{t}Bu) or $Sm(OAr)_2(THF)_3$ in toluene gave quantitatively the corresponding heteroleptic dimeric Sm(II) complexes $[(C_5Me_5)Sm(\mu\text{-}OAr)]_2$. The new complexes were characterized by their ^{1}H-NMR spectra, elemental analyses and melting points. The crystal structures were investigated by X-ray diffraction (Scheme 4).

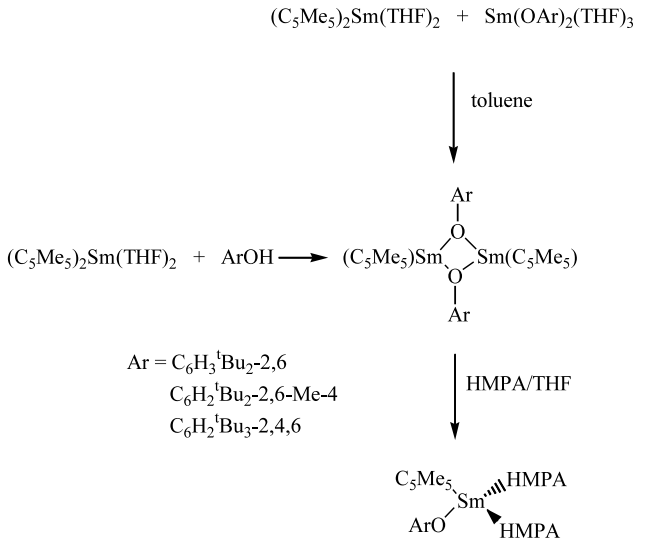

Scheme 4. Synthetic routes to unsolvated heteroleptic samarium(II) aryloxide/pentamethylcyclopentadienide complexes.

Besides alcoholysis the metathesis reaction between $Sm(OAr)_2$ with C_5Me_5K also afforded the heteroleptic samarium(II) aryloxide/pentamethylcyclopentadienyl complexes. The use of 2 equiv. of C_5Me_5K increased the yield of the product from 40 to 71%. In this reaction the product was coordinated with a neutral unit '$(\mu,\eta^5\text{-}C_5Me_5)K(THF)_2$'. The intermolecular $K\cdots C_5Me_5$ interactions constituted a polymeric structure in which each C_5Me_5 was bonded in a μ,η^5-fashion to a Sm atom on one side and to a K ion on the other side. The complex has a mirror plane, which is oriented along the polymer chain.

These complexes are stable in toluene solution and do not undergo ligand redistribution. Addition of 4 equiv. of hexamethyl phosphoric triamide (HMPA) to a THF solution afforded the corresponding HMPA-coordinated monomeric complexes (see Scheme 5). In the complex $[(C_5Me_5)Sm(\mu\text{-}OC_6H_2^tBu_3\text{-}2,4,6)]_2$ the two Sm atoms are bridged by two $OC_6H_2^tBu_3$-2,4,6-ligands and the $Sm(\mu\text{-}O)_2Sm$ unit is exactly planar. Both the Cp*- and the phenyl rings are almost perpendicular to the $Sm(\mu\text{-}O)_2Sm$ plane forming dihedral angles of 86 and 92° (Fig. 1).

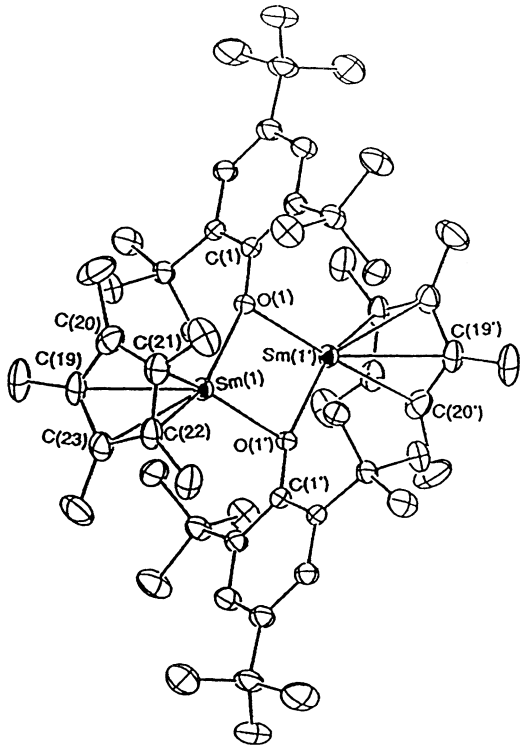

Fig. 1. ORTEP view of the molecular structure of $[(C_5Me_5)Sm\text{-}OC_6H_2^tBu_3\text{-}2,4,6]_2$.

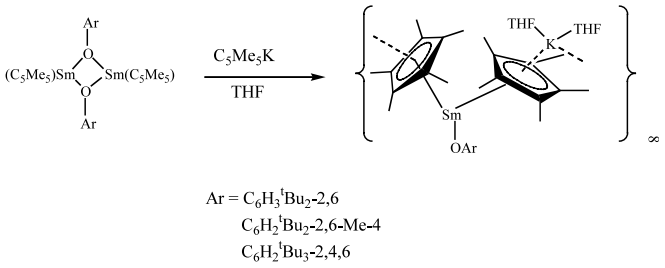

Scheme 5. Formation of the C_5Me_5K adduct of monomeric (C_5Me_5)-SmOAr.

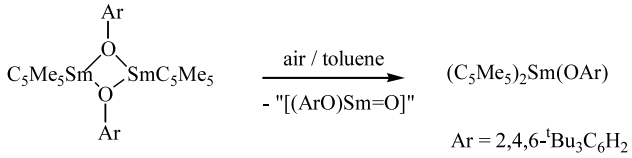

Scheme 6. Formation of $(C_5Me_5)Sm(OAr)$.

The complex possesses mirror symmetry. The Sm(1), O(1), C(1)–C(7), C(9)–C(11), C(13) and C(15) atoms are all located in this mirror plane and the two C_5Me_5 ligands are entirely eclipsed. Within the mirror plane, an agostic interaction between Sm and an *ortho*-^{t}Bu methyl group (C(9)) of the ArO ligand is observed. This agostic distance (3.055 Å) is comparable with the η^6-arene–Sm bond distances observed in the samarium(III) aryloxide complex $Sm_2(OC_6H_3^iPr_2\text{-}2,6)_6$.

When a green toluene solution of $[(C_5Me_5)SmOC_6H_2^tBu_3\text{-}2,4,6]_2$ was exposed to trace amounts of air, the trivalent samarium complex $[(C_5Me_5)SmOC_6H_2^tBu_3\text{-}2,4,6]$ was obtained in the form of orange–red crystals in 35% yield [2] (Scheme 6).

2.2.2. Bis(cyclopentadienyl) complexes

Casey et al. [3] reported the formation and characterization of an alkyl–alkene yttrium(III) complex. In situ prepared dimeric dicyclopentadienylyttrium hydride reacted rapidly with 3,3-dimethyl-1,4-pentadiene in methylcyclohexane-d_{14} at −78 °C and formed a bright yellow solution of the d^0 yttrium(III) pentenyl chelate complex $Cp_2^*Y[\eta^1,\eta^2\text{-}CH_2CH_2C(CH_3)_2\text{–}CH{=}CH_2]$ in 98 ± 5% yield. This pentenyl chelate complex was also prepared in toluene-d_8 in 84% yield. The chelate complex was stable for about 2 weeks at −78 °C but decomposed after a few hours at −50 °C (Scheme 7).

The complex was characterized without isolation by ^{1}H- and ^{13}C-NMR spectroscopy at −100 °C.

Mak and coworkers [4] synthesized five new bis(cyclopentadienyl)iodide complexes with lanthanum, samarium, yttrium, erbium and lutetium. The complexes were synthesized by halide exchange reactions between $[Cp''_2LnCl]_2$ and NaI in THF ($Cp'' = 1,3\text{-}(Me_3Si)_2C_5H_3$). The starting materials $[Cp''_2LnCl]_2$ were synthesized by treatment of anhydrous $LnCl_3$ with 2 equiv. of Cp″Na in THF. Subsequent treatment of $[Cp''_2LnCl]_2$ with excess of NaI at room temperature produced the organolanthanide iodide complexes $Cp''_2LnI(THF)$ in 50–69% yield.

The five monomeric complexes $Cp''_2LnI(THF)$ were fully characterized by elemental analysis, IR, MS, ^{1}H-NMR spectroscopy and single-crystal X-ray diffraction. In the complexes the metal atom is enclosed in distorted tetrahedral environment with the C_5 rings of Cp″, an oxygen atom of THF and an iodide ligand (Scheme 8).

Upon heating of Cp″LnI(THF) at 50 °C under vacuum the THF molecule was reversibly removable under formation of the dimeric complexes $[Cp''LnI]_2$. The iodo complexes have a dimeric structure similar to their chloro analogues.

The same authors also reported a more convenient and less time-consuming one-pot reaction method for making these iodide complexes. Cp″Na was added to a

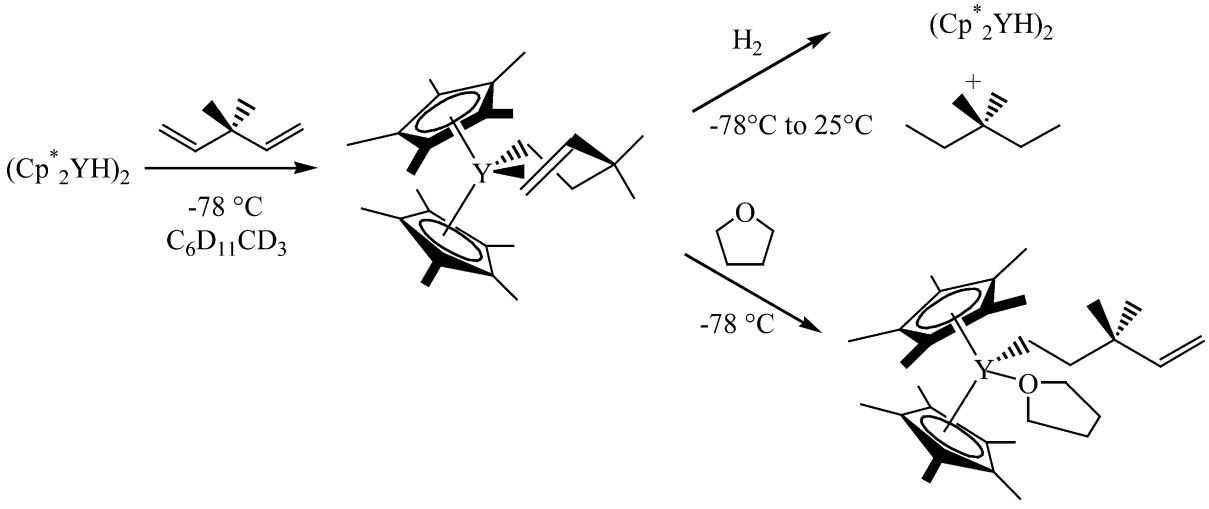

Scheme 7. Synthesis and reactions of $Cp_2^*Y[\eta^1,\eta^2\text{-}CH_2CH_2C(CH_3)_2\text{–}CH{=}CH_2]$.

$$2\ Cp''Na + LnCl_3 \xrightarrow{THF} 1/2\ [Cp''_2LnCl]_2 + 2\ NaCl$$

$$1/2\ [Cp''_2LnCl]_2 + NaI \xrightarrow{THF} Cp''_2LnI\ (THF) + NaCl$$

Ln = La, Sm, Y, Er, Lu

Scheme 8. Formation of the five monomeric complexes $Cp''_2LnI(THF)$.

$$2\ Cp''Na + LnCl_3 + NaI \xrightarrow{THF} Cp''_2LnI\ (THF) + 3\ NaCl$$

Scheme 9. One-pot reaction method for making the iodide complexes $Cp''_2LnI(THF)$.

$$Cp''Na + LuCl_3 \xrightarrow[-NaCl]{THF} Cp''LuCl_2(THF)_x + Cp'Na \xrightarrow[-NaCl]{THF}$$

$$[(Cp'')Cp'LuCl]_2 + NaI \xrightarrow[-NaCl]{THF} (Cp'')Cp'LuI(THF)$$

$Cp'' = 1,3\text{-}(Me_3Si)_2C_5H_3$; $Cp' = (Me_3Si)C_5H_4$

Scheme 10. Preparation of mixed π-ligand iodide complexes.

mixture of $LnCl_3$ and NaI in THF at room temperature (Scheme 9).

In the case of lutetium Mak and coworkers also prepared a mixed π-ligand iodide complex. The yield of this complex was lower than that of the lutetium complex containing two equal π-ligands [5] (Scheme 10).

All iodide complexes crystallized in the space group $P2_12_12_1$, and the metal atom in each complex has distorted tetrahedral coordination geometry (Fig. 2).

The mixed π-ligand iodide (Cp′)Cp″LuI(THF) crystallized in a lower symmetry than the lutetium iodide complex with two equal π-ligands (Fig. 3).

Voskoboynikov et al. [5] presented the crystal structure of $[(^tBuC_5H_4)_2Tb(\mu\text{-}Me)]_2$.

In this complex the metal atom adopts a tetrahedral geometry and the complex has C_{2h} symmetry (Fig. 4).

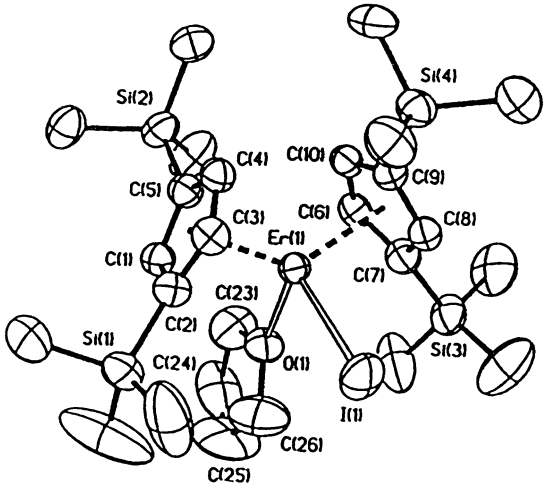

Fig. 2. ORTEP view of the molecular structure of $Cp''_2EuI(THF)$.

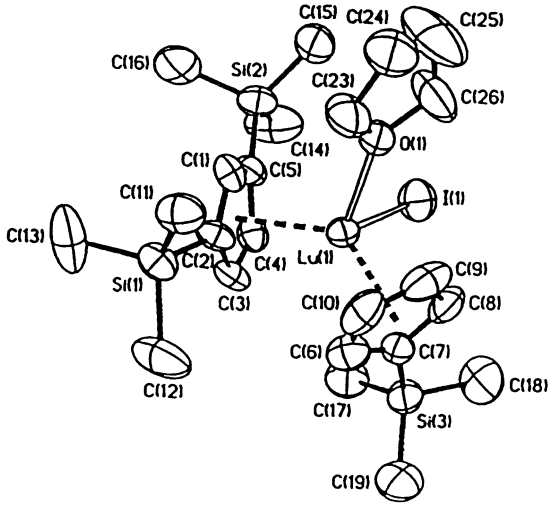

Fig. 3. ORTEP view of the molecular structure of (Cp′)Cp″LuI(THF).

Yttrium and lutetium hydrocarbyls react with various alkoxysilanes to produce the dimeric alkoxides $[Cp^*_2Ln(\mu\text{-}OR)]_2$ or the hydrocarbyl alkoxides $[Cp^*_2Ln(\mu\text{-}Me)(\mu\text{-}OR)]_2LnCp^*_2$ (R = Me, Et) depending on the reaction conditions. The reaction of $[Cp^*_2Lu(\mu\text{-}Me)]_2$ and $(MeOSi)_4$ provided only the hydrocarbyl alkoxide complex with a non-symmetrically bonded μ-OMe-ligand. The crystal structure of the complex $(^tBuC_5H_4)_2Lu(\mu\text{-}Me)(\mu\text{-}OMe)Lu\text{–}(^tBuC_5H_4)_2$ was investigated. The complex is binuclear and the Lu–OMe bridge distances (2.20(2) and 2.12(2) Å) and the Lu–O–C angles (122(1) and 129 (1)°) showed only small differences (Fig. 5).

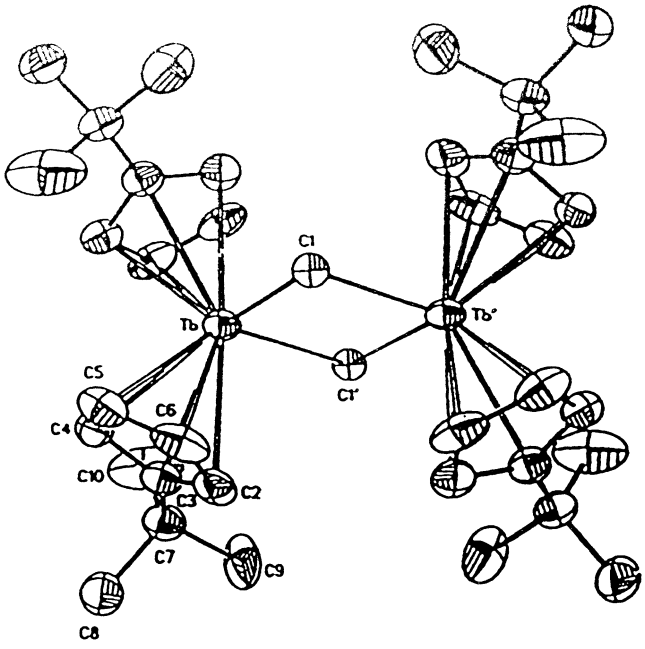

Fig. 4. ORTEP view of the molecular structure of $[(^tBuC_5H_4)_2Tb(\mu\text{-}Me)]_2$.

Baudry et al. [6] published the synthesis of unsolvated monomeric and dimeric samarium hydride complexes. The dimeric complex $[Cp'_2SmH]_2$ and monomeric $Cp'_2SmHBEt_3(THF)_n$ ($Cp' = C_5H_4^tBu$) trialkylborohydride were obtained from the starting dimeric $[Cp'SmCl]_2$ by reaction with the hydride reagent $NaHBEt_3$. A monomeric hydride, $Cp'_2SmH(PMe_3)_2$, was also obtained in the presence of a catalytic amount of PMe_3 by hydrogenolysis of Cp'_2SmR ($R = CH_2SiMe_3$ or $CH(SiMe_3)_2$). The trialkylborohydride was the most stable in solution as compared to other hydrides of samarium. All hydrides reacted with acetone to give the corresponding dimeric alkoxide derivative $[Cp'SmOCHMe_2]_2$.

The new alkyl complex $[Cp'_2SmMe]_2$ was isolated and characterized by NMR and elemental analysis (Scheme 11).

Shen and coworkers [7] published the synthesis of the (diisopropylamido)bis(methylcyclopentadienyl)lanthanides Ln = Y, Er, Yb. The complexes were synthesized in a two-step reaction and characterized by elemental analyses and IR spectroscopy Scheme 12.

The resulting lanthanide amides were subsequently reacted with a stoichiometric amount of phenylisocyanate. The first insertion product was isolated and the crystal structure was investigated (Ln = Y) (Scheme 13).

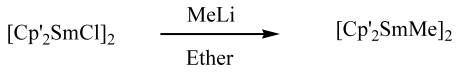

Scheme 11. Synthesis of $[Cp'_2SmMe]_2$.

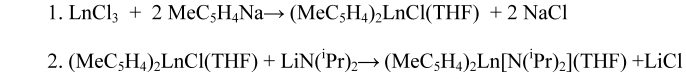

Scheme 12. Synthetic routes to leading to $(MeC_5H_4)_2Ln[N(^iPr)_2](THF)$.

The phenylisocyanate derived complexes $(MeC_5H_4)_2Ln(THF)[OCN(^iPr)_2NPh]$ Ln = Y, Er, Yb were characterized by their elemental analysis, IR, ^1H, ^{13}C, melting points and mass spectrometry.

Single crystals of the yttrium derivative $(MeC_5H_4)_2Y(THF)[OCN(^iPr)_2NPh]$ could be obtained from a concentrated toluene solution at −20 °C and were found to crystallize in the triclinic space group *P*1. The complex was monomeric and the yttrium atom was η^5-bonded to two methylcyclopentadienyl rings and additionally coordinated by one tetrahydrofuran and one bidentate ligand. The formal coordination number around the central metal Y is 9 (Fig. 6).

The N1–C1 distance is 1.323(5) Å and is thus slightly but significantly longer than the value accepted for a $N(sp^2)=C(sp^2)$ double bond (1.25 Å), and with 1.297(4) Å the O1–C1 distance is slightly but significantly shorter than that typical for a $O-C(sp^2)$ single bond with 1.324 Å. These bond parameters indicate some electronic delocalization over the O1–C1–N1 unit.

The authors also published a study of the catalytic activity of these (diisopropylamido)bis(methylcyclopentadienyl) lanthanides.

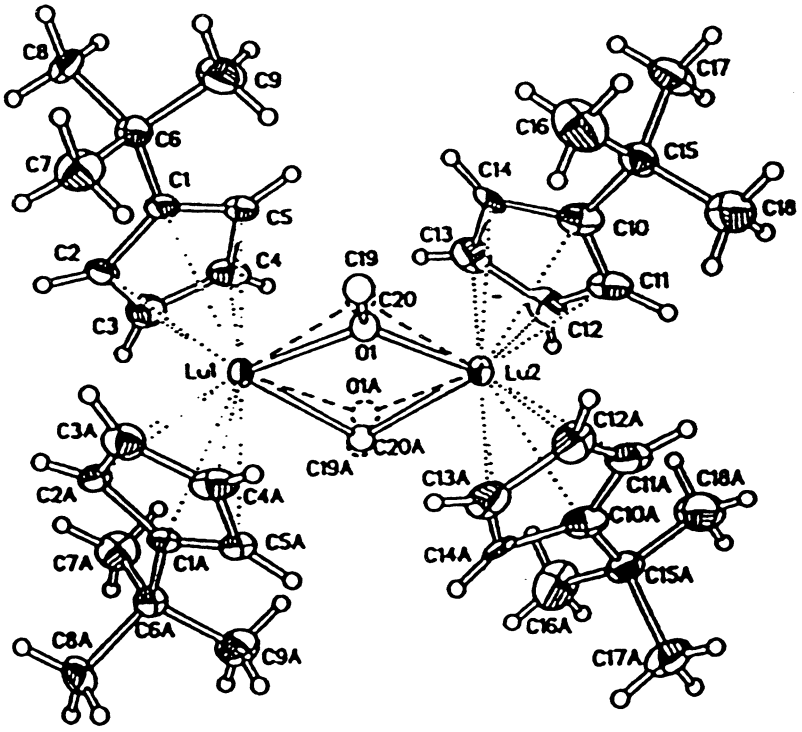

Fig. 5. ORTEP view of the molecular structure of $(^tBuC_5H_4)_2Lu(\mu\text{-}Me)(\mu\text{-}OMe)_2Lu(^tBuC_5H_4)_2$.

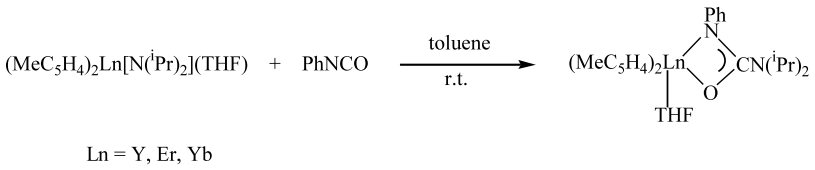

Scheme 13. Reaction of $(MeC_5H_4)_2[N(^iPr)_2](THF)$ with PhNCO.

Okuda and coworkers [8] synthesized chiral lanthanocene derivatives containing two linked amido-cyclopentadienyl ligands. They investigated their catalytic activity in lactone polymerization. These complexes containing a linked amido-cyclopentadienyl ligand would be ideal candidates for structurally defined initiators for the ring opening polymerization of lactones and related monomers. The reaction of 2 equiv. of dilithium amido-cyclopentadienide $Li_2(C_5R_4SiMe_2NCH_2CH_2X)$ ($C_5R_4 = C_5Me_4$, $C_5H_3^tBu$; X = OMe, NMe_2) with anhydrous $LnCl_3$ (Ln = Y, Lu) gave heterobimetallic complexes of the type $Li[Ln(\eta^5{:}\eta^1\text{-}(C_5R_4SiMe_2NCH_2CH_2X)_2]$. The complexes were characterized by their elemental analyses, ^1H- and ^{13}C-NMR as well as mass spectrometry. In the case of the complexes $Li[Y(\eta^5{:}\eta^1\text{-}(C_5Me_4SiMe_2NCH_2CH_2OMe)_2]$, (R,S)-$Li[Y(\eta^5{:}\eta^1\text{-}(C_5H_3^tBuSiMe_2NCH_2CH_2OMe)_2]$ and (R,R)-$Li[Y(\eta^5{:}\eta^1\text{-}(C_5H_3^tBuSiMe_2NCH_2CH_2NMe_2)_2]$ the molecular structures were determined by single-crystal X-ray analyses.

Ding and coworkers [9] reported the synthesis and characterization of a chiral bis(cyclopentadienyl)neodymium complex. $NdCl_3$ was reacted at first with 3.3 equiv. of NaCp in THF followed by subsequent treatment with (*S*)-(+)-*N*-(1-phenyl ethyl)salicylideneamine to afford the title compound (Scheme 14).

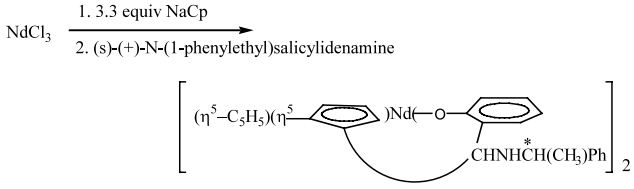

Scheme 14. Synthesis of chiral neodymium complex.

The product was obtained in 61% yield and characterized by elemental analysis (C, H, N and Nd) and IR spectroscopy as well as an X-ray structure analysis (Fig. 7).

2.2.3. *Ansa*-cyclopentadienyl complexes

Marks and coworkers [10] reported the synthesis and characterization of enantiomerically pure *ansa*-cyclopentadienyl organolanthanides $Me_2Si(^tBuCp)[(+)\text{-}neo\text{-}Men{-}Cp]Ln(CH(SiMe_3)_2$ and their use as precatalysts for asymmetric olefin hydrogenation.

In a one-pot reaction starting from 6,6′-dimethylfulvene, methyllithium and dimethyldichlorosilane the desired product $Me_2Si(^tBuCp)Cl$ was obtained, which was alkylated with Na[(+)-*neo*-Men–Cp] to afford the neutral ligand. Reaction with ^nBuLi afforded the dilithium salt as a colorless crystalline solid (Scheme 15).

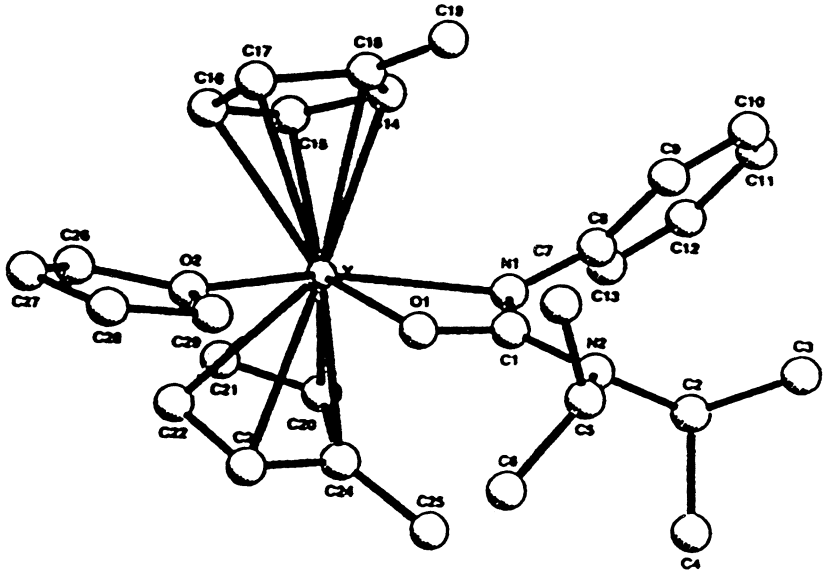

Fig. 6. ORTEP view of the molecular structure of $(MeC_5H_4)_2Y(THF)[OCN(^iPr)_2NPh]$.

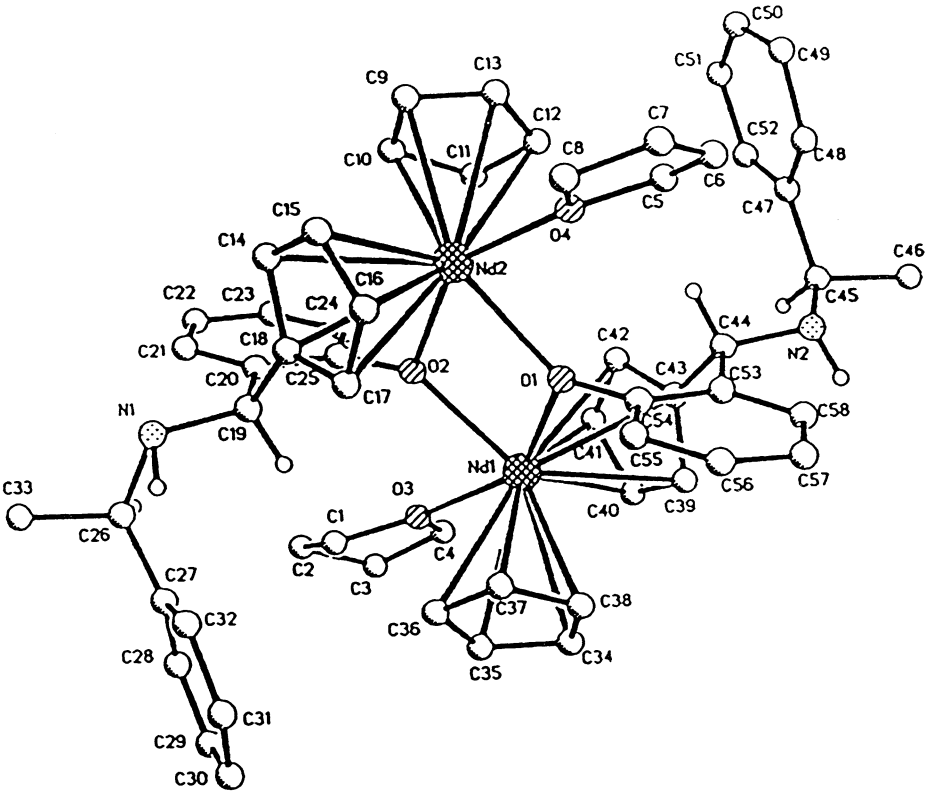

Fig. 7. ORTEP view of the molecular structure of the complex.

The synthesis of the corresponding organolanthanide chlorides was performed by trans-metalation of the dilithium salt with anhydrous lutetium or yttrium trichloride. Metallocene dichloro complexes (*R*,*S*)-$Me_2Si(^tBu–Cp)[(+)$-*neo*-Men–Cp]$Ln(\mu\text{-}Cl_2)Li(OEt_2)_2$ (Ln = Y, Lu) were synthesized by treatment of the

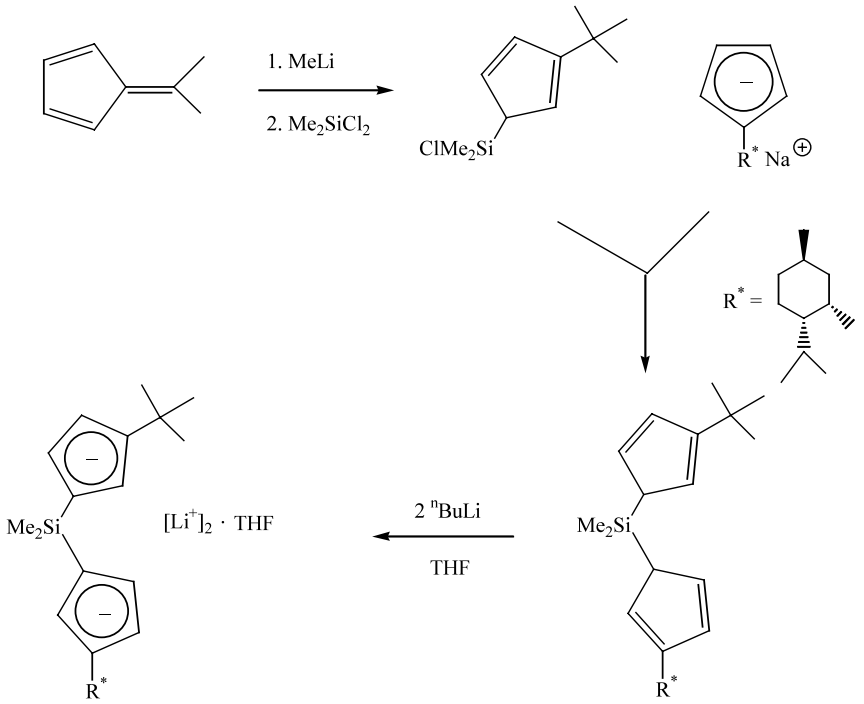

Scheme 15. Synthetic route leading to an enantiomerically pure *ansa*-cyclopentadienyl ligand.

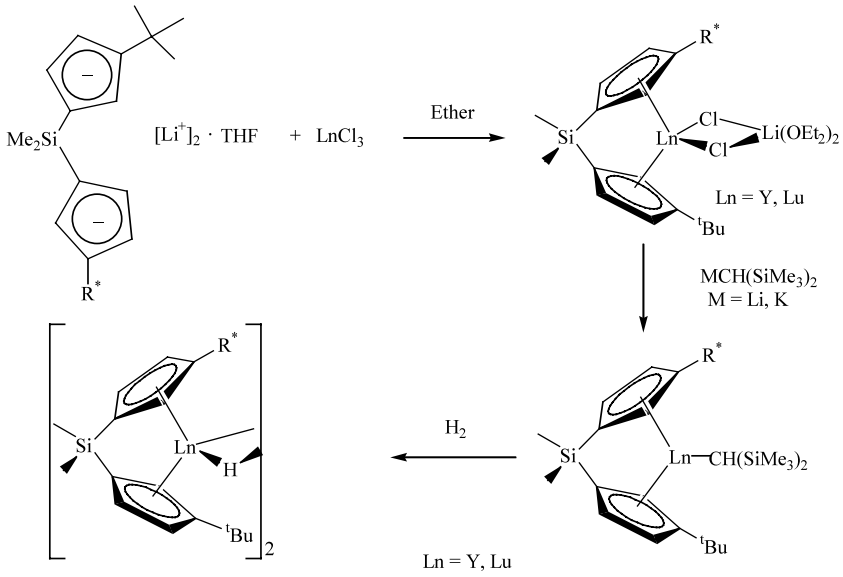

Scheme 16. Formation of the (*R*,*S*)-$Me_2Si(^tBu–Cp)[(+)$-*neo*-Men–Cp]$Ln(\mu\text{-}Cl_2)Li(OEt_2)_2$ complex and subsequent reactions.

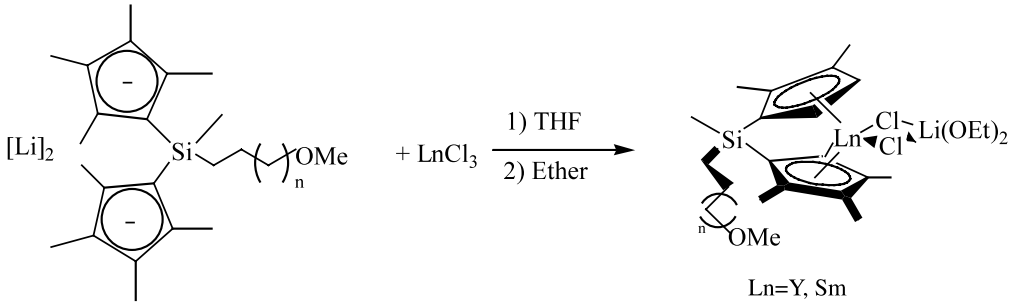

Scheme 17. Synthesis of tethered ether group functionalized *ansa* complexes $[R(Me)SiCp''_2]LnCH(SiMe_3)_2$.

corresponding lanthanide trichlorides with the dilithium salt of the ligand and were isolated isomerically pure by crystallization from diethyl ether (Scheme 16).

Marks and coworkers [11] also reported the synthesis and reactivity of other new *ansa*-cyclopentadienyl complexes. The new ligand is functionalized with a donor group, which is appended through varying chain length to the silicon bridge. The complexes $[R(Me)SiCp''_2]$–*LnCH*$(SiMe_3)_2$ (Ln = Y, Sm) were synthesized to investigate the influence of the tethered ether group on the reactivity and catalytic properties of the products (Scheme 17).

The ligand was synthesized in a 3-step reaction, and the key step of the ligand synthesis was the hydrosilylative fusion of the donor functionality R to the silicon center (Scheme 18).

2.2.4. Tris(cyclopentadienyl) complexes

A new synthetic method for preparing tris(pentamethylcyclopentadienyl) samarium was reported by Evans et al. [12] It involves reaction of tetramethylfulvene with the dimeric samarocene hydride $[(C_5Me_5)_2Sm(\mu\text{-}H)]_2$ (Scheme 19).

The reagent of $[(C_5Me_5)_3Sm(\mu\text{-}H)]_2$ was in turn produced by the reaction of $[(C_5Me_5)_3Sm]$ and H_2 under hydrogenolysis. This product was characterized by ^{1}H-NMR spectroscopy (Scheme 20).

Hanusa and coworkers [13] reported the use of alkaline-earth metallocenes $(C_5Me_5)_2Ca(THF)_x$ (x = 0–2) as cyclopentadienyl ring metathesis (CRM) reagents with lanthanide and the main group metal complexes. The CRM reaction provided a controllable route to mixed-ring cyclopentadienyl species and allowed to study the effect of changes in the ligand environment around a metal center in a systematic manner. The type of product formed was depending on whether unsolvated or solvated lanthanocene derivatives were employed.

In the CRM reaction between unsolvated lanthanocene and $[Ca(C_5Me_5)_2]$ 50% of excess of the coreagent was used to overcome the low solubility of $[Ln(C_5H_5)_3]$ in toluene. The excess did not generate any $[Ln(C_5Me_5)_3]$ but $[Ln(C_5Me_5)_2(C_5H_5)]$ (Scheme 21).

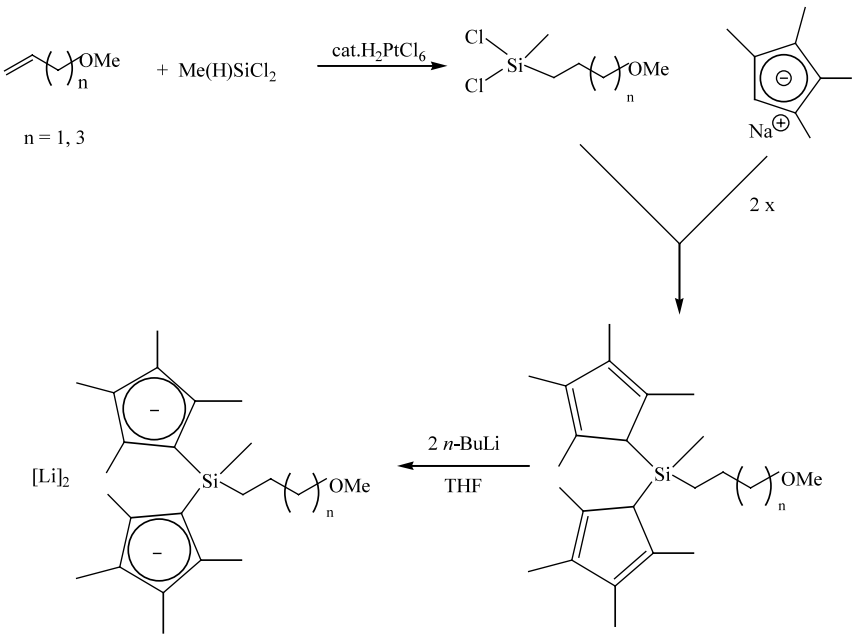

Scheme 18. Synthesis of the *ansa*-cyclopentadienyl complexes with a donor group.

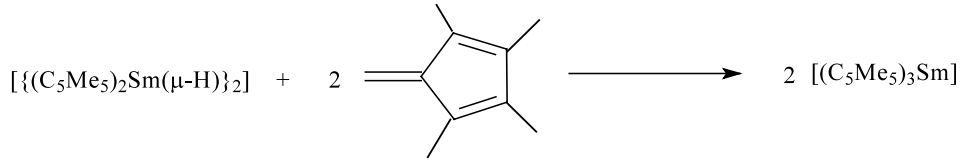

Scheme 19. Preparation of tris(pentamethylcyclopentadienyl)samarium by hydrogenation of tetramethylfulvene.

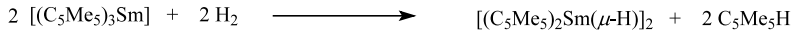

Scheme 20. Formation of $[(C_5Me_5)_2Sm(\mu\text{-}H)]_2$.

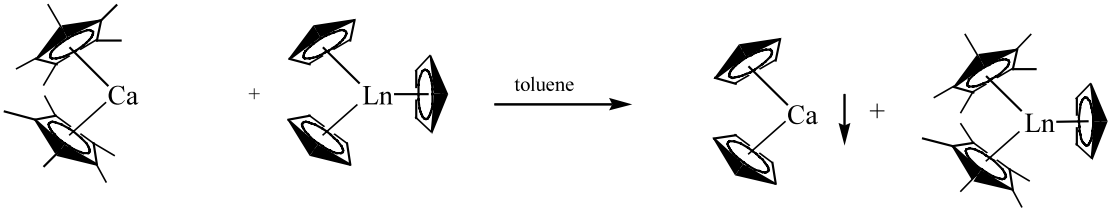

Scheme 21. Synthesis of THF-free lanthanocene by the CRM reaction.

The CRM reaction took an appreciably different course when solvated starting materials were used. Only one $[C_5Me_5]^-$ exchange at the lanthanide centre was observed (Scheme 22).

When $K[C_5Me_5]$ was reacted with $[Ln(C_5H_5)_3(THF)_{1.5}]$ in excess or in three times more than the equimolar ratio, no $[C_5Me_5]^-$ ring transfer to the lanthanum centre was observed.

The products were characterized by elemental analyses, IR, ^{1}H-, and ^{13}C-NMR spectroscopy.

Amberger and coworkers [14] investigated the electronic structure of organometallic complexes, especially η^5-cyclopentadienyl complexes of the *f*-elements. Because of the polymeric nature of the base-free Cp_3Ln compounds, they focused on monomeric homoleptic cyclopentadienyl lanthanide complex of the type Cp_3La using sterically demanding substituted η^5-cyclopentadienyl ligands such as $(Me_3SiC_5H_4)^-$ and $[1,3\text{-}(Me_3Si)_2C_5H_3]$. For example, the molecular structure of the complex $[1,3\text{-}(Me_3Si)_2C_5H_3]_3Ce$ displays a pseudo-trigonal planar geometry. The CF splitting pattern of $(Me_3SiC_5H_4)_3Pr$ was obtained on the basis of absorption, magnetic circular dichroism (MCD) and luminescence measurements. By fitting the experimental

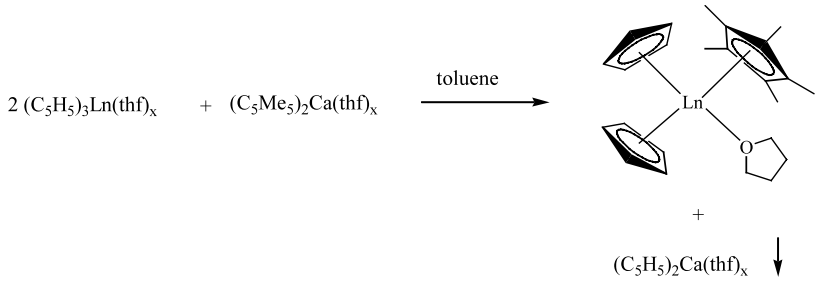

Scheme 22. Formation of lanthanocenes in the CRM reaction with solvated starting materials.

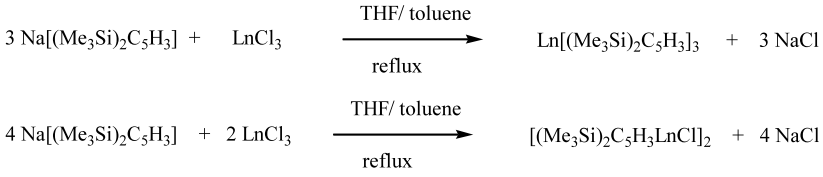

Scheme 23. Formation of $[(Me_3Si)_2C_5H_3]_3Ln$ and $[(Me_3Si)_2C_5H_3LnCl]_2$.

parameters of an empirical Hamiltonian the authors obtained the splitting pattern and could estimate the CF strength of $Me_3SiC_5H_4$-ligand.

Xie et al. [15] investigated the formation of di- and triorganolanthanide complexes dependent on the size of the central metal. Anhydrous lanthanide trichlorides were refluxed with an excess amount of Na[$(Me_3Si)_2C_5H_3$] (NaCp″). For the metals La, Nd, Sm, Gd, and Dy tris(ligand) complexes of the type [$(Me_3Si)_2C_5H_3]_3Ln$ and for the metals Gd, Dy, Y, Er, and Yb bis(ligand) complexes of the type [$\{(Me_3Si)_2C_5H_3\}_2LnCl]_2$ were formed (Scheme 23).

It is interesting to mention that neither THF-coordinated complexes nor THF ring-opened products of the type $Cp''_2LnO(CH_2)_4Cp''(THF)$ were formed. Also no tris(ligand) complex was isolated for Ln = Y, Er or Yb. The compounds were fully characterized by elemental analyses, IR, MS and ^{1}H-NMR spectroscopy. The melting points of Cp''_3Ln were lower than those of $[Cp''LnCl]_2$. The structures of the complexes [$(Me_3Si)_2C_5H_3]_3La$, $[(Me_3Si)_2C_5H_3]_3Nd$, $[(Me_3Si)_2C_5H_3]_3Gd$ and $[(Me_3Si)_2C_5H_3]_3Dy$ have been determined by single crystal X-ray analysis. They all crystallized in a monoclinic space group and each of the $(Me_3Si)_2C_5H_3$ ligands was η^5-bonded to the central lanthanide atom to form a trigonal planar geometry with an average (ring centroid)–metal–(ring centroid) bond angle of 120° (Fig. 8).

2.2.5. Complexes with cyclopentadienyl and cyclooctatetraenyl ligands

Edelmann and coworkers [16] reported the preparation of three new mono(cyclopentadienyl)/mono(cyclooctatetraenyl) sandwich complexes of lanthanides with Ln = Pr, Sm, Tb. The complexes (COT*)Ln(Cp″) (COT* = 1,4-$(Me_3Si)_2C_8H_6^{2-}$; Cp″ = 1,3-$(Me_3Si)_2-C_5H_3^-$) have been synthesized in a one-pot reaction by simultaneous treatment of anhydrous lanthanide trichlorides with equimolar amounts of Li_2COT^* and LiCp″. The complexes were characterized by IR, ^{1}H-, ^{29}Si-NMR and elemental analyses (Scheme 24).

2.3. Complexes with indenyl ligands

Hanusa and coworkers [14] attempted to synthesize lanthanum indenyl complexes using the CRM reactions. They took equimolar amounts of $[Ln(C_5H_5)_3(THF)_{1.5}]$ and K[Ind] and obtained a mixture of starting materials

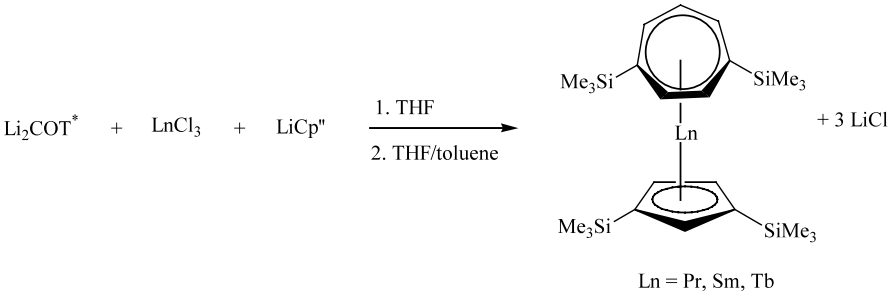

Scheme 24. Synthesis of mono(cyclopentadienyl)/mono(cyclooctatetraenyl)lanthanide complexes.

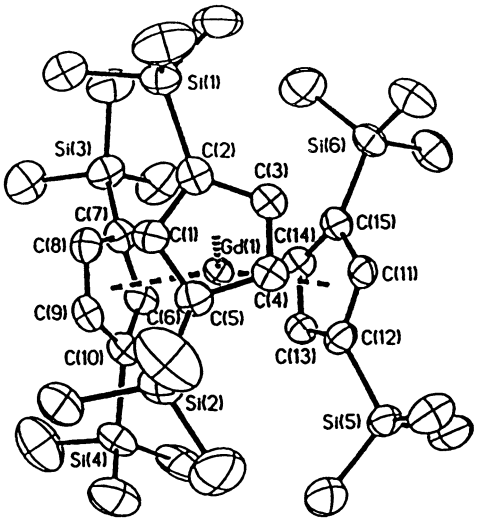

Fig. 8. ORTEP view of $[(Me_3Si)_2C_5H_3]_3Gd$.

and $[Ln(Ind)_{3-n}(C_5H_5)_n(THF)]$, $n = 0$, 1, 2. Similar results were obtained in the reaction between $[Ln(C_5H_5)_3(THF)]$ and $[Ca(Ind)_2(THF)_2]$.

Shen et al. [17] published the synthesis of indenyl complex of praseodymium and lanthanum. Upon treatment of anhydrous $PrCl_3$ with $Na(C_9H_7)$ in a 1:2 and $LaCl_3$ with $Na(C_9H_7)$ in a 1:3 molar ratio in THF the indenyl complexes were formed. In the complex $[(C_9H_7)_2PrCl(THF)]_2$ the central praseodymium is surrounded by two indenyl, two Cl and one THF ligand in a bipyramidal arrangement. The average distances Pr–C(ring) are 2.81 and Pr–Cl 2.84 Å (Fig. 9).

In the complex $(C_9H_7)_3La(THF)$ the central lanthanum is surrounded by three indenyl and one THF ligand in a pseudo-tetrahedral arrangement (Fig. 10).

Huang and coworkers [18] published two new binuclear bis(indenyllanthanide) alkoxides, $[(C_9H_7)_3Ln(\mu, \eta^2\text{–}OCH_2CHCH_2CH_2CH_2)]_2$ with Ln = Nd, Pr. These new complexes have been characterized by IR, mass spectrometry and metal analysis. The tris(indenyl)lanthanide complexes $(C_9H_7)_3Ln(THF)$ reacted with equimolar amounts of 2-tetrahydrofurfuryl methanol at room temperature to afford the binuclear bis(indenyl)lanthanide alkoxides. The crystal structure of the Nd complex showed that the oxygen atoms of the tetrahydrofurfuryl methoxide ligand act as both a bridging and a chelating group in the complex. The Nd atom is coordinated by two η^5-C_9H_7 rings, two oxygen atoms of tetrahydrofurfuryl methoxide ligands and an oxygen atom of a tetrahydrofuran ring to give the formal coordination number 9. The Nd–C(η^5-C_9H_7) distances range from 2.79(2) to 2.92(2) Å and the Nd–O(1)(μ-OR′) bond distances are 2.30(1) and 2.31(1) Å. In the intermolecular five-membered chelating ring the Nd–O(2) distance is 2.51(1) Å (Fig. 11).

Fischer and coworkers [19] investigated the crystal structure of four homologous tris(indenyl)lanthanide(THF)-adducts of the type $(C_9H_7)_3Ln(THF)$ with Ln = La, Pr, Nd, Sm. Some structural differences in the conformations were found for these molecules. The C_5-fragments of the C_9H_7 ligands are almost *penta-hapto*-bonded, and either two or three C_9H_7 units adopt paddlewheel-like orientations. The complexes with La and Nd contain dimorphic crystals. Except the samarium complex, the crystals contain two molecules of different conformations. Three characteristic structural motifs I, II and III were found. Motif I which is realized in the La, Pr, and Nd-complexes is particularly complicated in that each crystal involves two non-equivalent molecular conformations *a* and *b*. In the molecular conformation all indenyl ligands lie paddlewheel-like and in the molecular conformation *b* only two indenyl ligands are in the paddlewheel arrangement.

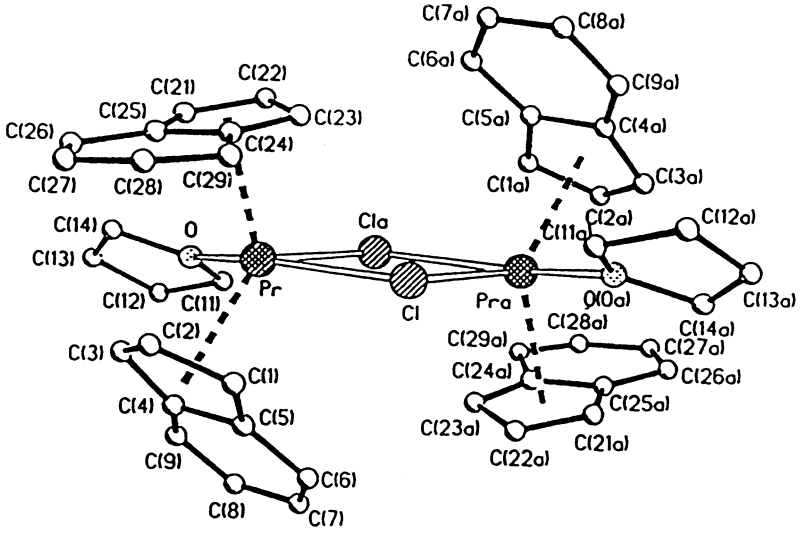

Fig. 9. ORTEP view of the molecular structure of $[(C_9H_7)_2PrCl(THF)]_2$.

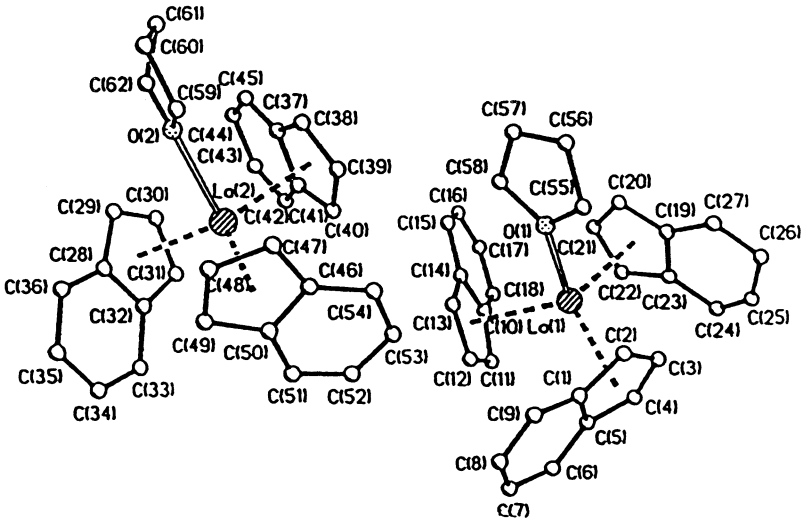

Fig. 10. ORTEP view of the molecular structure $(C_9H_7)_3La(THF)$.

Motif II showed only one type of molecule. All three indenyl ligands were orientated in a different way. One of them lies almost equatorial (i.e. paddlewheel-like), the second axial and the third one in an essentially intermediate position. In the motif III the three indenyl ligands enclosed the Ln^{3+} ion clockwise in the equatorial plane.

2.4. Complexes with cyclooctatetraenyl ligands

Amberger and coworkers [20] synthesized (COT)Nd-^{III}[HB(3,5-Me_2pz)$_3$] and investigated the electronic feature of the COT-ligand in this complex. They measured the absorption spectrum at different temperatures, and the bands were assigned by applying the selection rules for C_{8v} symmetry. The CF parameters found for $[COT]^-$ were the same as in the praseodymium case.

2.5. Complexes with heteroatom five-membered ring ligands

Xie et al. [21] published the synthesis and characterization of *closo*- and exo-*nido* lanthanide carboranes. They treated anhydrous $LaCl_3$ and SmI_2, respectively, with 1 equiv. of Na_2[7,8-R_2–*nido*-7,8-$R_2C_2B_9H_9$], R = H, $C_6H_5CH_2$ and obtained the colorless sandwich complexes *closo*-[$(THF)_2$Na][$(R_2C_2B_9H_9)_2$La$(THF)_2$] and dark red dimeric exo-*nido*-[{$(C_6H_5CH_2)_2C_2B_9H_9$}-Sm$(DME)_2]_2$·DME complex. The complexes were characterized by their ^{1}H-, ^{13}C-, ^{11}B-NMR, IR, and complexometric metal analyses, and their crystal structures were confirmed by X-ray analysis (Scheme 25, Fig. 12).

It is noteworthy that no desired half-sandwich mono(dicarbollide)lanthanum species was isolated. The La ion is η^5-bonded to the pentagonal C_2B_3 face of each

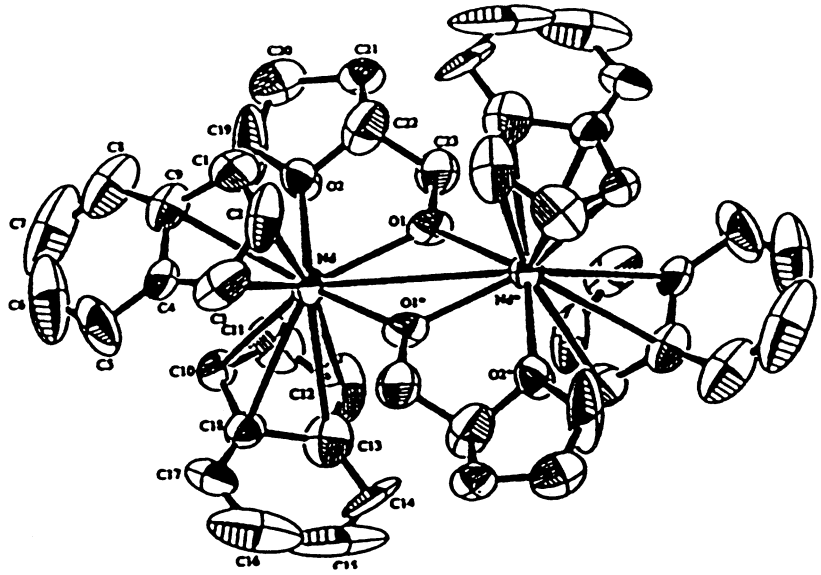

Fig. 11. ORTEP view of the molecular structure of $[(C_9H_7)_3Ln(\mu, \eta^2\text{–}OCH_2CHCH_2CH_2CH_2)]_2$.

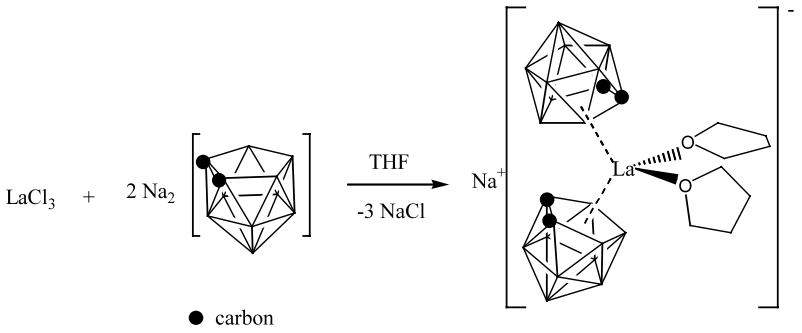

Scheme 25. Formation of $\{R_2C_2B_9H_9)_2La(THF)_2\}^-$.

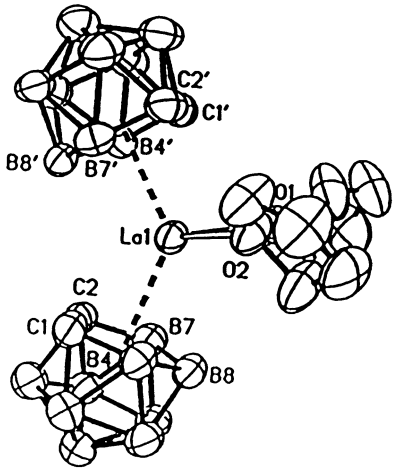

Fig. 12. ORTEP view of the molecular structure of the anion $[(R_2C_2B_9H_9)_2La(THF)_2]^-$.

of the two dicarbollide cages and two coordinated THF molecules in a distorted tetrahedral coordination geometry. The average La–cage atom average distance is 2.804(5) Å and this value is comparable with the La–C distances for other eight-coordinated η^5-pentamethylcyclopentadienyl lanthanum complexes.

Treatment of SmI_2 with an equimolar amount of $Na_2[7,8\text{-}(C_6H_5CH_2)_2$–*nido*-7,8-$C_2B_9H_9]$ in THF at room temperature accompanied by a solvent exchange from THF to DME gave the complex $[\{(7,8\text{-}(C_6H_5CH_2)_2)$–*nido*-7,8-$C_2B_9H_9\}Sm(DME)_2]_2(DME)$ (Scheme 26, Fig. 13).

The complex crystallized in the orthorhombic space group *Pbcn*. In the dimeric samarium complex each of the two dibenzyldicarbollide ligands served as a bridging ligand for two samarium atoms. The main feature of this structure is the presence of exclusive Sm–H–B-bonding between Sm(II) and dibenzyldicarbollide anions. This is the first example of a structurally characterized exo-*nido*-lanthanacarborane of the C_2B_9 system.

2.6. Organolanthanide complexes in organic synthesis

Ishii and coworkers [22] discovered that $Cp^*_2Sm(thf)_2$ catalyzes the regioselective acylation of tertiary alcohols under acid-free conditions in the presence of an oxime ester. Scheme 27 illustrates the supposed catalytic process.

Scheme 27 illustrates that the alcohol reacts with the oxime ester in the presence of $Cp^*_2Sm(thf)_2$ to produce the ester and cyclohexanone oxime which subsequently reacts with isopropenyl acetate to regenerate cyclohexanone oxime acetate.

As already mentioned in Section 2.1, several new compounds of cerium were synthesized and investigated as addition reagents in organic synthesis. Table 1 shows the results of enantioselective addition reactions of organocerium reagents with 2-methyl-3-vinylcyclopentanone (Scheme 28).

2.7. Organolanthanide catalysis

Voskoboynikov et al. [5] reported the results of reactions between lanthanide (Ln = Tb, Yb, Lu, Y) hydrocarbyls and various organosilicon, -germanium, -tin, -aluminum and -gallium hydrides in hydrocarbon solution. The reaction did not produce the expected compounds with lanthanide-element bonds but the corresponding unsolvated dimeric lanthanide and yttrium hydrides $[Cp^*_2Ln(\mu\text{-}H)]_2$. The progress of the reaction between $PhMeSiH_2$ and $[Cp^*_2Lu(\mu\text{-}Me)_2]_2$ and $PhMeSiH_2$ $[Cp^*_2Y(\mu\text{-}Me)_2]_2$ was followed by ^{1}H-NMR spectroscopy at 20 °C. Thus it was demonstrated that the dihydrido complexes of lanthanides were formed via

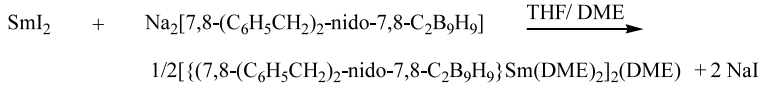

Scheme 26. Synthesis of the complex $[\{(7,8\text{-}(C_6H_5CH_2)_2)$–*nido*-7,8-$C_2B_9H_9\}Sm(DME)_2]_2(DME)$.

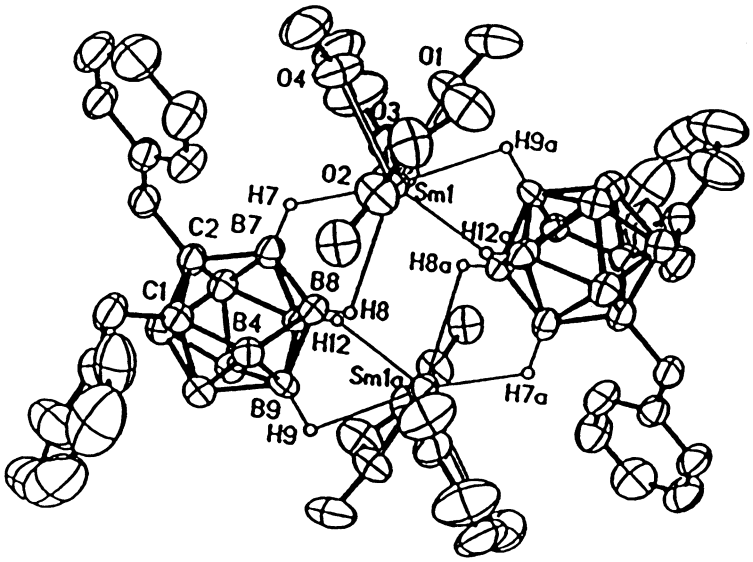

Fig. 13. ORTEP view of the molecular structure of the dimeric complex $[\{(C_6H_5CH_2)_2C_2B_9H_9\}Sm(DME)_2]_2$.

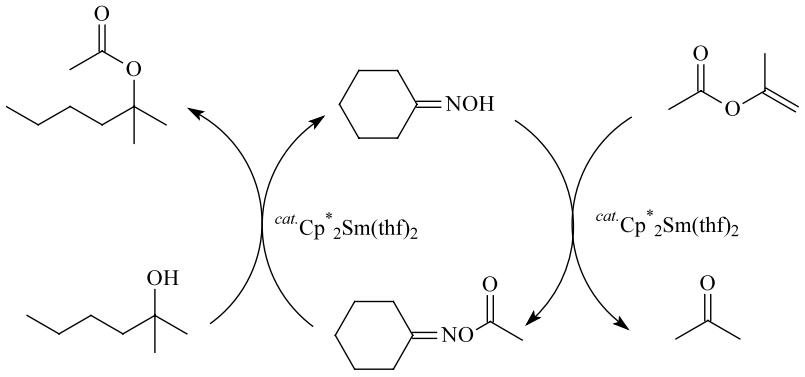

Scheme 27. Postulated reaction path of the $Cp^*_2Sm(THF)_2$-catalyzed acylation of 2-methyl-2-hexanol.

Table 1
Reactions of organocerium reagents with 2-methyl-3-vinylcyclopentanone

No.	Reagents	ee (%)	Yield (%)	Enolization (%)
1	MeLi	10	65	22
2	$MeLi/CeCl_3$	68	91	–
3	$MeLi/Ce(NEt_2)_3$	78	55	25
4	$MeLi/Ce(N^iPr_2)_3$	79	50	36
5	$MeLi/Ce(O^iPr_2)_3$	83	95	–
6	$MeLi/Ce(O^iPr_2)_3$ [a]	86	93	–
7	$MeLi/Ce(O^iPr_2)_3$ [b]	74	90	–
8	$MeLi/ClCe(O^tBu)_2$	77	85	–
9	$MeLi/ClCe(OCH^iPr_2)_2$	87	89	–
10	^{n}BuLi	49	56	36
11	^{n}BuLi/$ClCe(OCH^iPr_2)_2$	89	90	–
12	^{t}BuLi	77	35	57
13	^{t}BuLi/$ClCe(OCH^iPr_2)_2$	90	80	–
14	PhLi	85	70	24
15	PhLi/$ClCe(OCH^iPr_2)_2$	94	95	–

[a] Addition at −98 °C.
[b] In Et_2O.

intermediates containing both μ-Me and μ-H bridges. Dimeric compounds of the type $[Cp^*_2Ln(\mu\text{-}H)(\mu\text{-}Me)\text{–}LnCp^*_2]$ with different bridging ligands were isolated. This reaction is a convenient and effective method for the synthesis of yttrium and lanthanide hydrides. The same authors also investigated the reactivity of lanthanide hydrides toward organosilicon hydrides and related compounds. The catalytic reaction of dimeric yttrium hydrides in the H/D exchange reaction in silanes was reported (Scheme 29).

Evans et al. [12] described the initiation of ethylene polymerization caused by $(C_5Me_5)_3Sm$. The activity of sterically overcrowded $(C_5Me_5)_3Sm$ was unexpected, because in this complex there is no potential center of activity like Sm(II), hydride or alkyl. The initiation of ethylene polymerization was supposed to proceed through a η^1-C_5Me_5-intermediate of $(C_5Me_5)_3Sm$ (Scheme 30).

Evans et al. [23] also investigated the alkylation system $LnCl_3/RLi$. Until now '$RLnCl_2$' was written as

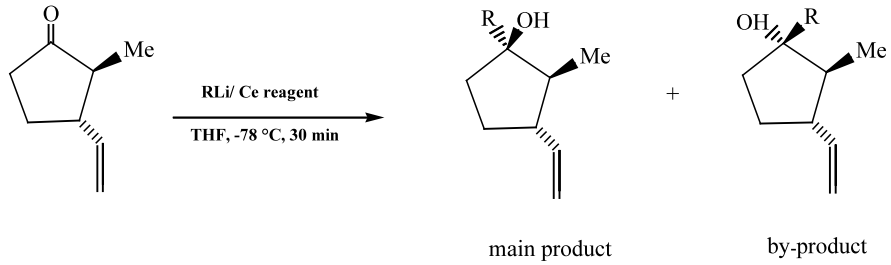

Scheme 28. Enantioselective addition reactions of organocerium reagents with 2-methyl-3-vinylcyclopentanone.

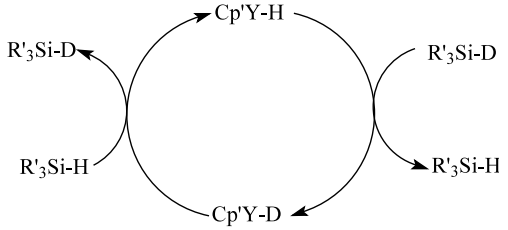

Scheme 29. H/D exchange reaction between yttriumhydrides and silanes.

the active species, but the general drying method for preparing anhydrous $CeCl_3$ did not remove all solvated water and lead to monosolvated $[CeCl_3(H_2O)]_n$. This complicated the reaction since at least some of the RLi could react with the water to form $Ce_aCl_bR_c(OH)_dO_eLi_f$. To determine the precise nature of the $[CeCl_3(H_2O)]_n$/RLi diamagnetic ^{89}Y was used as a model. The anhydrous YCl_3 was obtained by the usual method of dehydrating by heating. Recrystallization at 25 °C from a THF solution gave crystals of $[YCl_2(H_2O)_6]Cl$.

As already mentioned in Section 2.2.3, Marks and coworkers [10] reported an investigation of asymmetric hydrogenation of unfunctionalized olefins by enantiomerically pure organolanthanides of the type (*R*,*S*)-$Me_2Si(^tBuCp)[(+)$-*neo*-Men–Cp]LnCH$(SiMe_3)_2$ (Ln = Y, Lu). These complexes represent a second generation of asymmetric organolanthanide catalysts employing a new type of potentially pseudo-C_2-symmetric ligation and the results of this study offer an interesting contrast to the other known classes of diastereomerically pure asymmetric organolanthanide catalysts. The unfunctionalized olefins are typically difficult substrates to hydrogenate/deuterate with substantial enantioselectivity (Scheme 31).

In the frontal approach of the olefin, the large substituent (L) of the olefin would be oriented *syn* to the ^{t}Bu substituent and *anti* to the bulkier (+)-neomenthyl group. The *ee* values obtained for 1-pentene were up to 63%.

Novak and coworker [24] reported the synthesis of 'link-functionalized' (LFP) poly(methyl methacrylate) (PMMA) and poly(ε-caprolactone) (PCL) using bimetallic complexes of the type $(C_5Me_5)_2Sm–R–Sm(C_5Me_5)_2$. Bis-initiated polymerization of methyl methacrylate and ε-caprolactone through the bimetallic complexes $(C_5Me_5)_2Sm–R–Sm(C_5Me_5)_2$ gave polymers with discrete functionalities at the center of the backbone, the LFP polymers (Scheme 32).

LFP's are of special interest because:

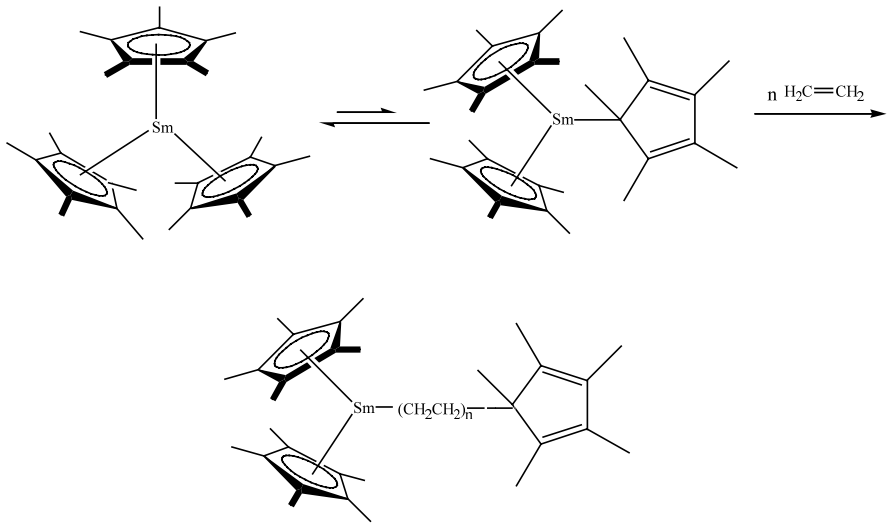

Scheme 30. Equilibrium between $(C_5Me_5)_3Sm$ and $(C_5Me_5)_2Sm–\eta^1$-C_5Me_5 and insertion of ethylene.

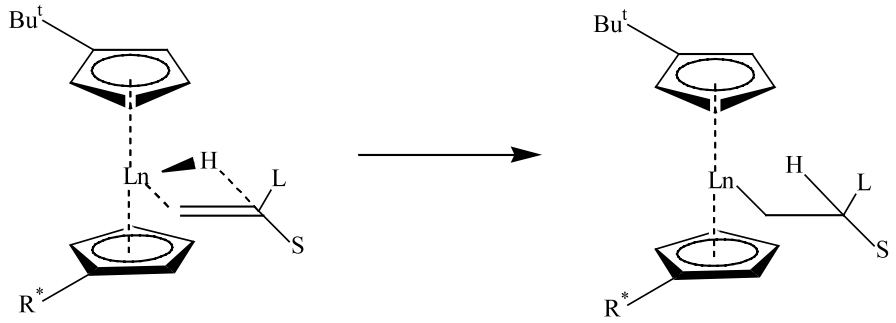

L=large substituent, S=small substituent

Scheme 31. Enantioselective hydrogenation of unfunctionalized olefins with large (L) and small (S) substituents.

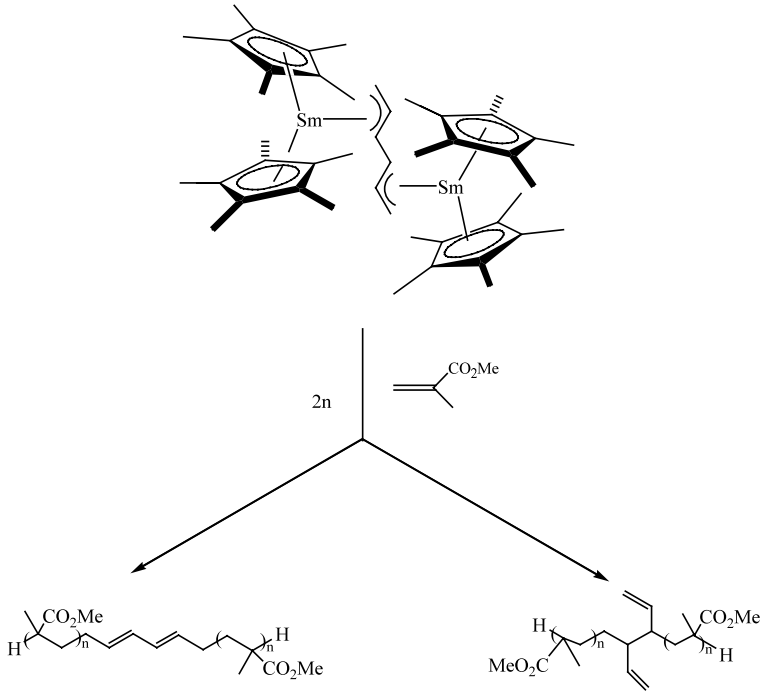

Scheme 32. Synthesis of olefin-functionalized PMMA.

– LFP's may serve as building blocks to other architectures.
– LFP's are useful models for the environment experienced by the polymer backbone, and the LFP functionality may be used to influence the polymerization process itself (Scheme 33).

As already mentioned in Section 2.2.2, Shen and coworkers [7] synthesized lanthanide amides of the type $(MeC_5H_4)_2Ln(THF)[OCN(^iPr)_2NPh]$, Ln = Y, Er, Yb, and tested their activity in the polymerization of PhNCO. The result of polymerization for the complex $(MeC_5H_4)_2Y(THF)[OCN(^iPr)_2NPh]$ at 30 °C showed a good activity and yielded yellow solid polymers when 300 equiv. of PhNCO were added. The polymers consisted of 43% methanol-insoluble and 57% methanol-soluble fractions.

Okuda and coworkers [8] investigated the ring-opening polymerization of ε-caprolactone catalyzed by the heterobimetallic complexes $Li[Ln(\eta^5{:}\eta^1\text{-}C_5R_4SiMe_2NCH_2CH_2X)_2]$. The product of this polymerization had a high molecular weight $M_n > 30\,000$ and moderate polydispersity ($M_w/M_n < 2.0$). The polymerization was carried out in toluene or dichloromethane at room temperature. The results are summarized in Table 1. The lutetium complex was found to be the least effective catalyst. The homoleptic tris(amide) $Y[N(SiMe_3)_2]_3$ was also found to polymerize ε-caprolactone.

As the initial step of the polymerization, one can anticipate a nucleophilic attack by one of the nucleophilic amido-nitrogen atoms at the lactone carbonyl-

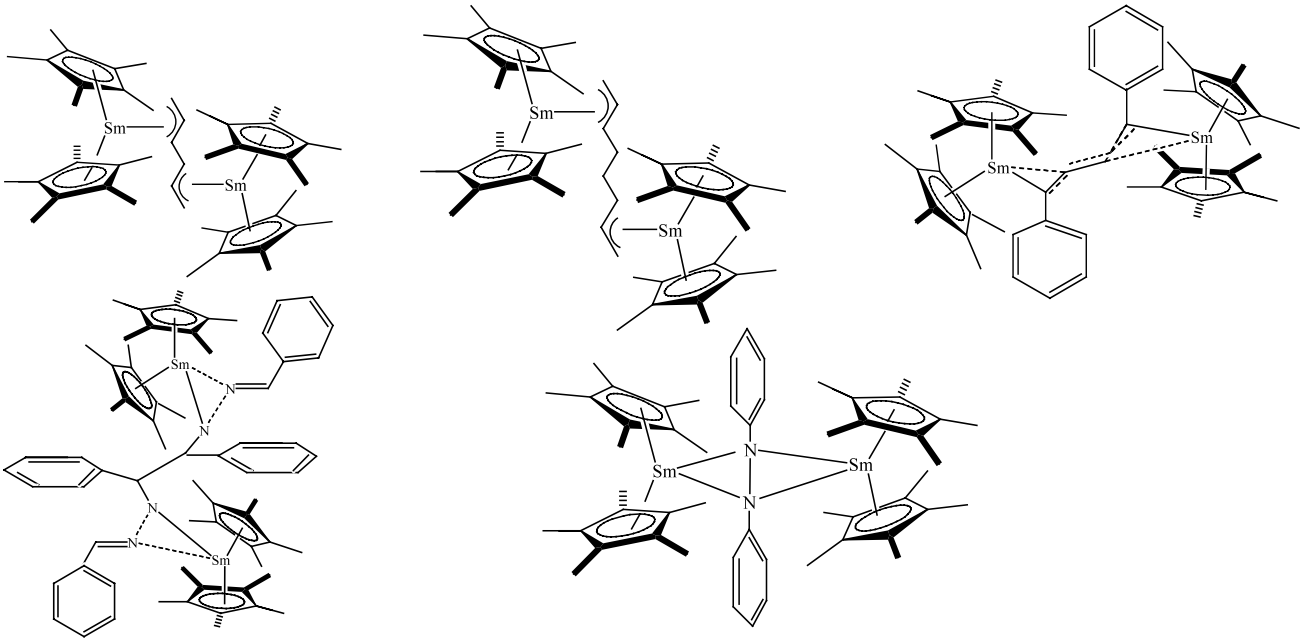

Scheme 33. Five bimetallic Sm(II) initiators.

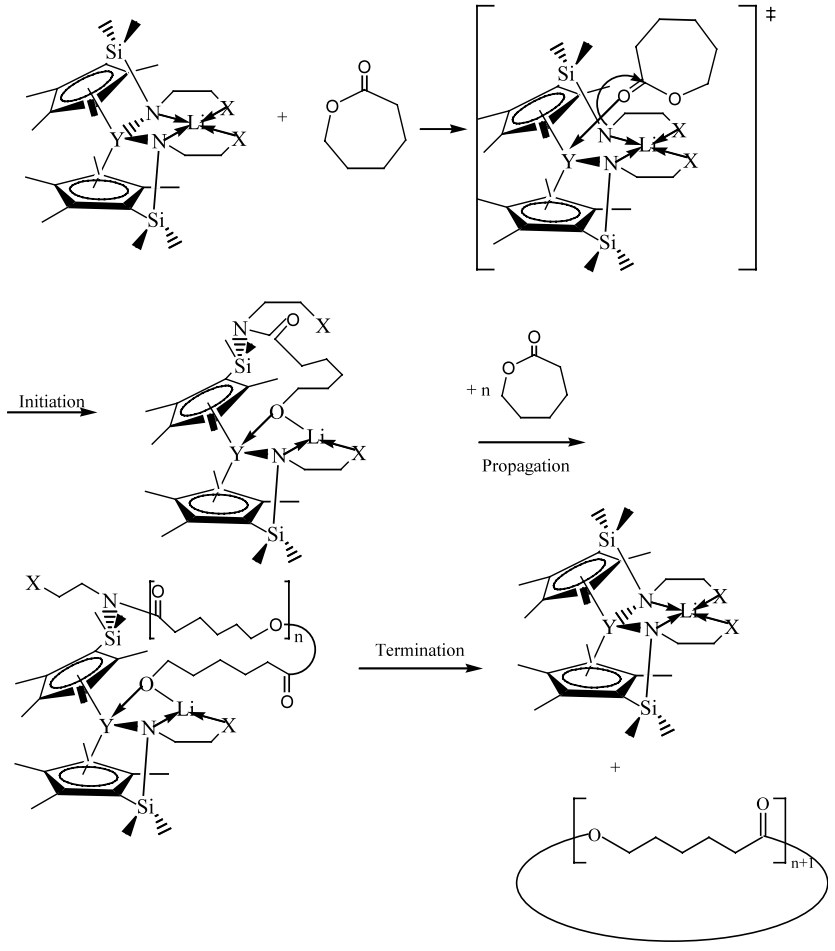

Scheme 34. Ring-opening polymerization of ε-caprolactone catalyzed by the heterobimetallic complexes $Li[Ln(\eta^5{:}\eta^1\text{-}(C_5R_4SiMe_2NCH_2CH_2X)_2]$.

carbon atom, followed by acyl bond cleavage and formation of an alkoxide (Scheme 34, Table 2).

Molander et al. [25] published the selective sequential cyclization/silylation of 1,6- and 1,7-enynes by the organoyttrium complex $Cp^*YCH_3(THF)$. They also described the catalytic mechanism in a detailed manner (Scheme 35).

It was proposed that the catalytic cycle is initiated by σ-bond metathesis between $Cp^*_2YCH_3(THF)$ and $PhSiH_3$, producing a catalytically active metal hydride species 'Cp^*_2YH'. In the next step, the catalyst inserts preferentially at the alkyne sites. This intermediate undergoes cyclization via an intramolecular olefin insertion and produces a second intermediate alkyl yttrium species. In the reaction with silane this intermediate undergoes a subsequent σ-bond metathesis to generate the cyclized product.

Marks an coworkers [26] reported the $Cp'_2Ln/Me_2SiCp''_2Ln$-catalyzed hydrogenation of acyclic imines to yield the corresponding amines (Scheme 36).

The stoichiometric reaction of *N*-benzylidene-(methyl)amine with $Cp^*_2SmCH(SiMe_3)_2$ or $(Cp^*_2SmH)_2$ yields an ortho-metalated Cp'_2Sm-substrate complex which undergoes either hydrogenolysis/hydrogenation or competing C=N insertion of a second substrate molecule to yield a Cp^*_2Sm–imine–amido complex with a seven-membered chelate ring (Scheme 37).

The stoichiometric reaction of 2-methylen-1-pyrroline results in the formation of a Cp^*_2Sm–imine–amido complex in with two substrate molecules have been coupled to form a six-membered chelate ring (Scheme 38, Fig. 14).

The stoichiometric reaction of *N*-benzylidene(trimethylsilyl)amine with $(Cp^*_2SmH)_2$ yields a Cp^*_2Sm–imine–amido complex with a four-membered $Sm(NSiMe_3)(CPh)N{=}CHPh$ chelate ring. Heating of this product under H_2 gave S_6-symmetric $(Cp^*_2SmCN)_6$, which contains an unusual chair-like 18-membered $(SmCN)_6$ ring.

3. Actinides

3.1. Complexes with cyclopentadienyl ligands

3.1.1. Bis(cyclopentadienyl) complexes

Rabinovich et al. [27] reported the synthesis and crystal structure determination of bis(η^5-pentamethylcyclopentadienyl)thorium(IV) dibromide complex $Cp^*_2ThBr_2$ [$Cp^* = \eta^5$-C_5Me_5]. $ThBr_4(THF)_4$ was allowed to react with 2.2 equiv. of $Cp^*MgCl{\cdot}THF$ to give the title complex.

Rabinovich et al. [28] also reported the synthesis and characterization of the first dicarbollide thorium complexes. A THF suspension of $ThCl_4$ or a THF solution of $ThCl_4(TMEDA)_2$ was reacted with 2 equiv. of lithium dicarbollide ($Li_2C_2B_9H_{11}$) to form the anionic bis(dicarbollide) complex $[Th(\eta^5\text{-}C_2B_9H_{11})_2Cl_2]^{2-}$. By fractional

Table 2
Polymerization of ε-caprolactone catalyzed by heterobimetallic complexes [a]

Initiator	Time (h)	Solvent	[Monomer]/[cat]	Yield (%)	M_n($\times 10^3$) (g mol^{-1})	M_w($\times 10^3$) (g mol^{-1})	M_w/M_n
Li[**Y**(η^5:η^1-$C_5Me_4SiMe_2NCH_2CH_2$**O**Me)$_2$] [b]	1.5	Toluene	42	85	58	112	1.9
Li[**Y**(η^5:η^1-$C_5Me_4SiMe_2NCH_2CH_2$**O**Me)$_2$]	1.5	Toluene	90	78	34	53	1.6
Li[**Y**(η^5:η^1-$C_5Me_4SiMe_2NCH_2CH_2$**O**Me)$_2$]	1.5	Toluene	147	82	44	67	1.5
Li[**Y**(η^5:η^1-$C_5Me_4SiMe_2NCH_2CH_2$**O**Me)$_2$] [c]	1.5	Toluene	188	92	177	333	1.9
Li[**Y**(η^5:η^1-$C_5Me_4SiMe_2NCH_2CH_2$**O**Me)$_2$]	1.5	Toluene	197	92	39	72	1.8
Li[**Y**(η^5:η^1-$C_5Me_4SiMe_2NCH_2CH_2$**O**Me)$_2$]	1.5	CH_2Cl_2	183	75	14	19	1.4
Li[**Y**(η^5:η^1-$C_5Me_4SiMe_2NCH_2CH_2$**N**Me$_2$)$_2$]	1.5	Toluene	199	94	94	159	1.7
Li[**Lu**(η^5:η^1-$C_5Me_4SiMe_2NCH_2CH_2$**O**Me)$_2$]	5	Toluene	221	42	14	16	1.1
Li[**Lu**(η^5:η^1-$C_5Me_4SiMe_2NCH_2CH_2$**O**Me)$_2$]	42	CH_2Cl_2	180	89	11	14	1.3
Li[**Y**(η^5:η^1-$C_5H_3'BuSiMe_2NCH_2CH_2$**O**Me)$_2$] [d]	1.5	Toluene	220	92	76	135	1.8
Li[**Y**(η^5:η^1-$C_5H_3'BuSiMe_2NCH_2CH_2$**O**Me)$_2$] [e]	1.5	Toluene	245	91	51	83	1.6
Li[**Y**(η^5:η^1-$C_5H_3'BuSiMe_2NCH_2CH_2$**N**Me$_2$)$_2$] [f]	1.5	Toluene	246	91	31	50	1.6
Li[**Y**(η^5:η^1-$C_5H_3'BuSiMe_2NCH_2CH_2$**N**Me$_2$)$_2$] [g]	1.5	Toluene	230	89	80	141	1.8
Y[N(SiMe$_3$)$_2$]$_3$	1.5	Toluene	224	65	524	1509	2.9

[a] [cat] = 5×10^{-3} mol l^{-1}.
[b] [cat] = 42×10^{-3} mol l^{-1}.
[c] [cat] = 10×10^{-3} mol l^{-1}.
[d] (*R*,*R*)–(*R*,*S*) = 1:6.
[e] (*R*,*R*)–(*R*,*S*) = 1.7:1.
[f] (*R*,*R*)–(*R*,*S*) = 1:5.
[g] (*R*,*R*)–(*R*,*S*) = 3.5:1.

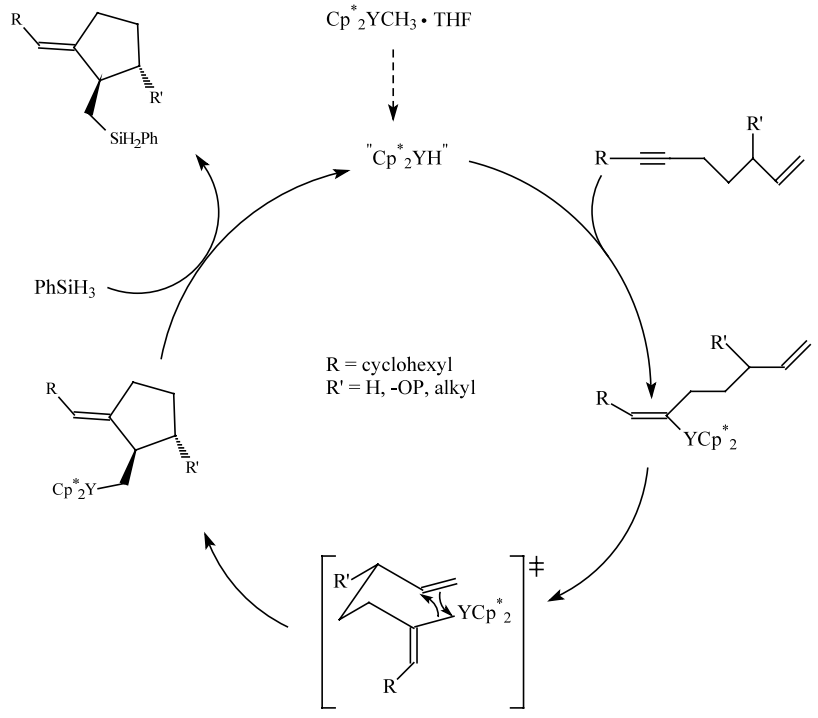

Scheme 35. The selective sequential cyclization/silylation of 1,6-enynes by $Cp^*_2YCH_3(THF)$.

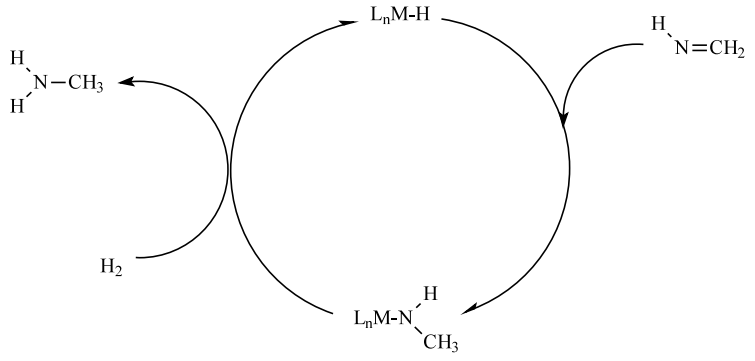

Scheme 36. Organolanthanide-catalyzed imine hydrogenation.

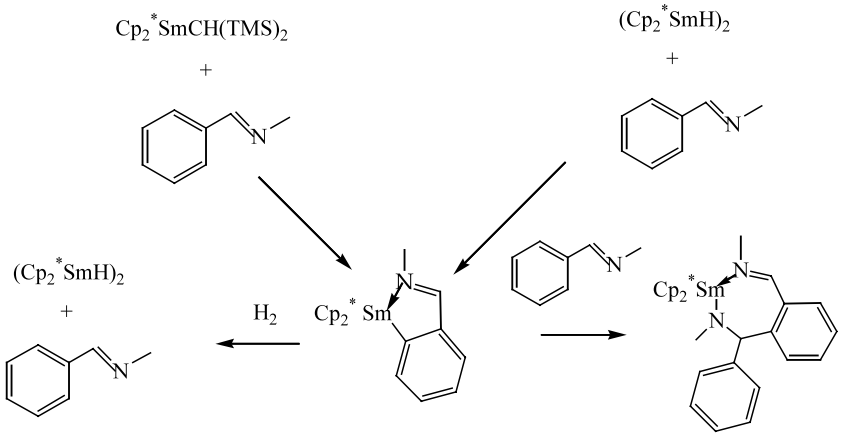

Scheme 37. Reaction of *N*-benzylidene(methyl)amine with $Cp^*_2SmCH(TMS)_2$.

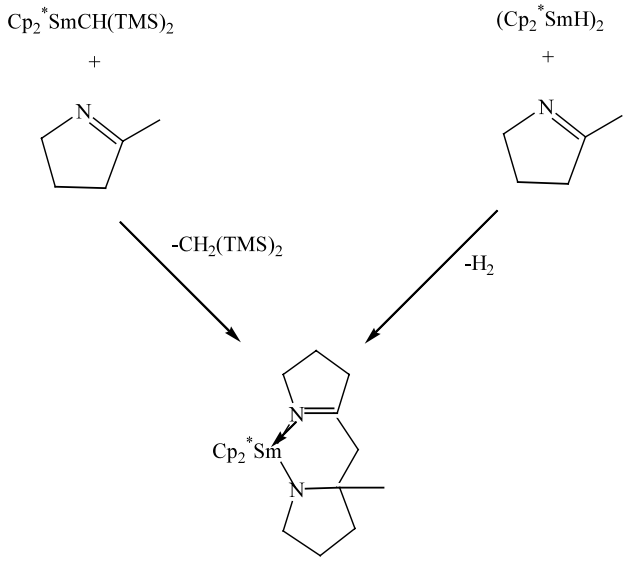

Scheme 38. Reaction of 2-methylpyrroline with organosamarium complexes.

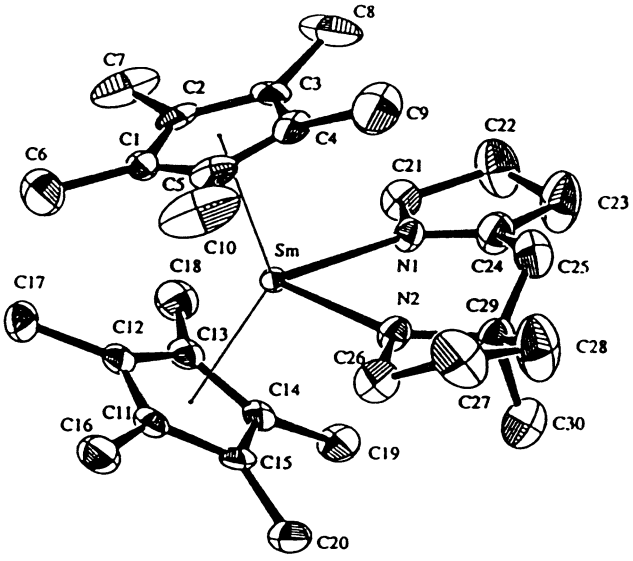

Fig. 14. ORTEP view of the molecular structure of $Cp_2^*Sm(C_{10}H_{18}N_2)$.

crystallization the lithium salt of the complex was isolated in a yield of 39%. The yield of the corresponding bromo complex was 75% (Scheme 39, Fig. 15).

Ephritikhine and coworkers [29] studied the reactivity of the cationic uranium compound $[Cp_2^*U(NMe_2)(THF)][BPh_4]$. Treatment of this uranium complex with ^{t}BuNC afforded the isocyanide adduct $[Cp_2^*U(NMe_2)(CN^tBu)_2][BPh_4]$, whereas reactions with MeCN, CO_2 and CO gave the insertion compounds $[Cp_2^*U\{NC(Me)(NMe_2)\}(THF)][BPh_4]$, $[Cp_2^*U(O_2CNMe_2)(THF)][BPh_4]$ and $[Cp_2^*U(\eta_2\text{-}CONMe_2)(THF)][BPh_4]$ (Scheme 40).

The compounds were characterized by their IR and ^{1}H-NMR spectra as well as their elemental analyses. The crystal structure of $[Cp_2^*U(NMe_2)(CN^tBu)_2][BPh_4]$

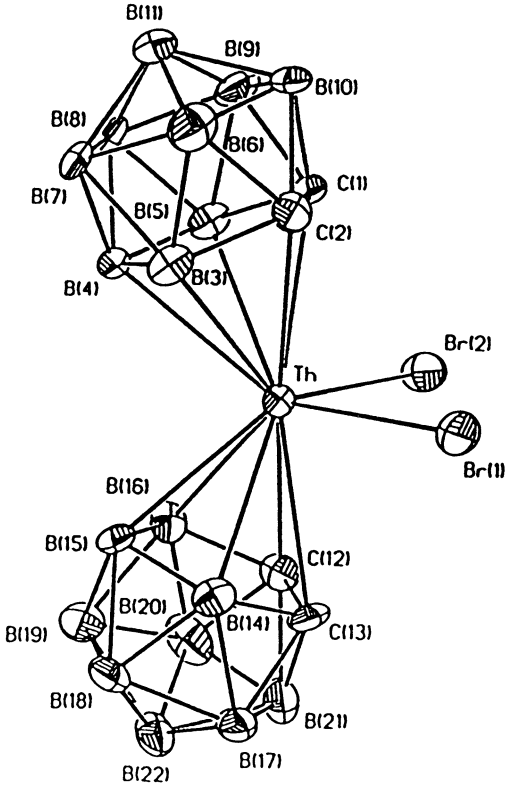

Fig. 15. ORTEP view of $[Th(\eta^5\text{-}C_2B_9H_{11})_2Cl_2]^{2-}$.

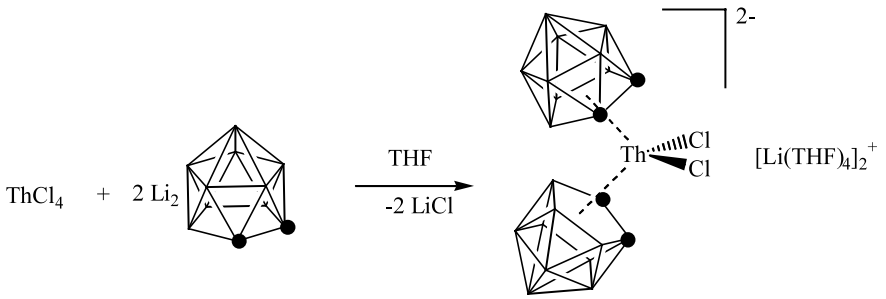

Scheme 39. Synthesis of $[Th(\eta^5\text{-}C_2B_9H_{11})_2Cl_2]^{2-}$.

has been determined. It consists of discrete cation–anion pairs. The cation $[Cp^*_2U(NMe_2)(CN^tBu)_2]^+$ adopts the classical bent sandwich structure of $[(\eta\text{-}C_5R_5)_2M(X)_2(Y)]$ compounds. The arrangement of the amide and two isocyanide ligands in the equatorial girdle is symmetrical (Fig. 16).

The U, N(3), C(21) and C(26) atoms are coplanar and this plane is almost perpendicular to that defined by U, N(3) and the two centroids of the Cp* rings. The C(21)–U–C(26) angle 152.5° is similar to the Cl–U–Cl angle 151.0° in $[Cp^*_2U(Cl)_2(HNPPh_3)]$. The uranium–nitrogen distance of 2.22 Å is in the range of U–N bond lengths for terminally coordinated amide ligands and the geometry of the UNC_2 fragment is planar; these structural parameters are indicative of a π-interaction between the U and N atoms.

3.1.2. Tris(cyclopentadienyl) complexes

Evans et al. [12] published the first tris(pentamethylcyclopentadienyl) complex of uranium. This complex was synthesized by hydrogenation of tetramethylfulvene with $(C_5Me_5)_2UH(dmpe)$. The yield of this complex was 50% and the complex was characterized by common analytical methods (IR, ^{1}H-, ^{13}C-NMR, magnetic susceptibility and elemental analysis) (Scheme 41, Fig. 17).

$U(C_5Me_5)_3$ crystallizes isostructurally with $Sm(C_5Me_5)_3$. In the uranium complex there are three different bond lengths with an average length of 2.84(4) Å, but the angles between the three Cp* ligands are exactly 120°. The three Cp* ligands are orientated in such a way that the sterical interaction between them is minimized.

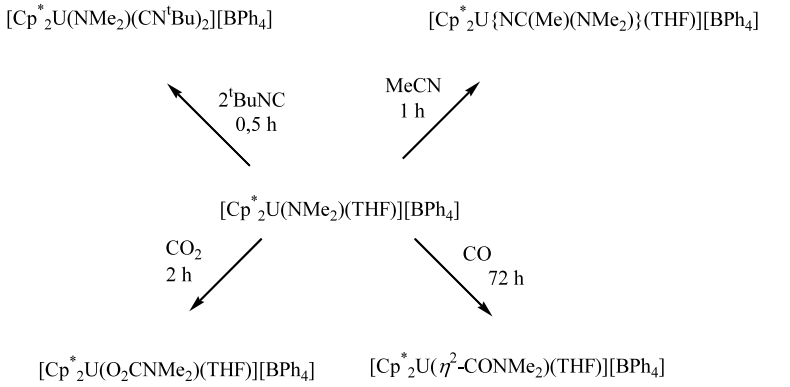

Scheme 40. Reaction of the uranium amide complex $[Cp^*_2U(NMe_2)(THF)][BPh_4]$ with unsaturated molecules.

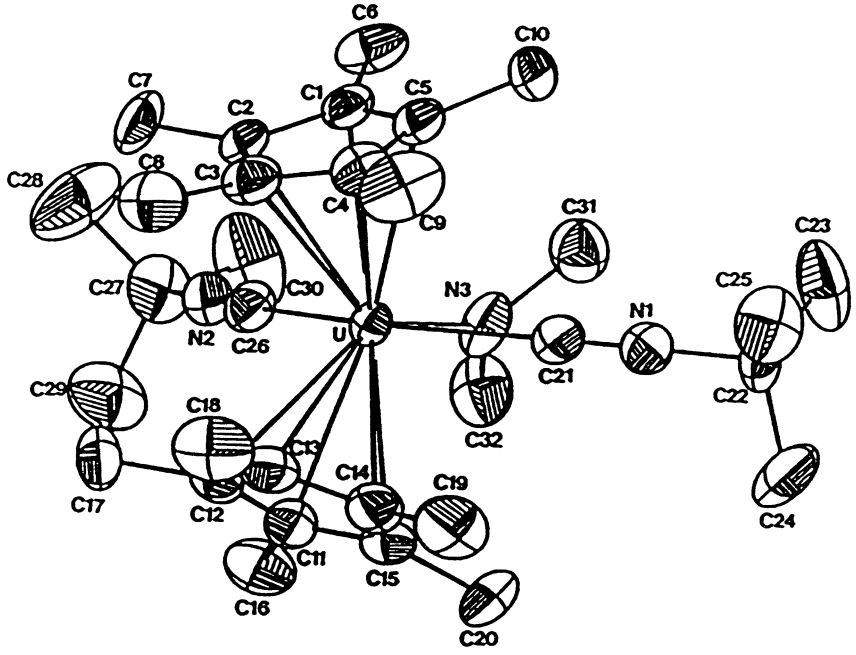

Fig. 16. ORTEP view of the molecular structure of $[Cp^*_2U(NMe_2)(CN^tBu)_2][BPh_4]^+$.

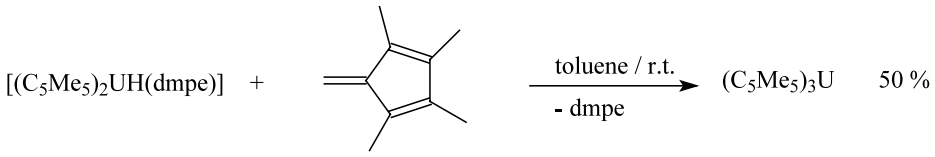

Scheme 41. Hydrogenation of 1,5-tetramethylfulvalen leads to tris(pentamethylcyclopentadienyl)uranium.

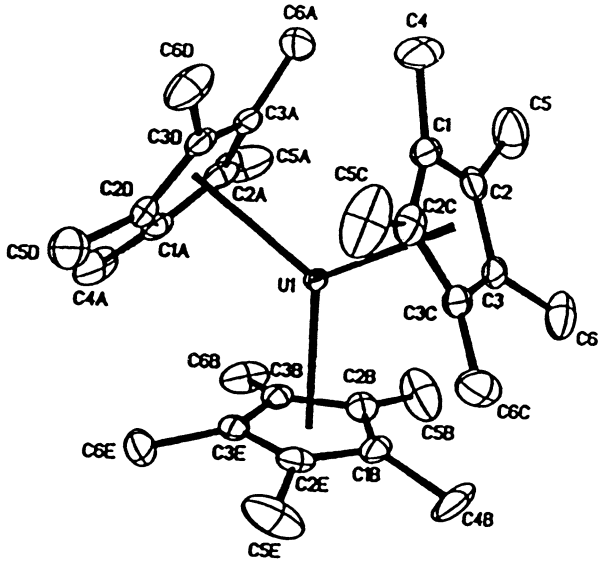

Fig. 17. ORTEP view of molecular structure of $U(C_5Me_5)_3$.

3.2. Complexes with pentalene ligands

Cloke and Hitchcock [30] published the synthesis of a new class of actinide 'sandwich' complexes with pentalene ligands. Tris(alkylsilyl) substituted pentalene rings act like the η^8-membered ring system cyclooctatetraenyl. The dipotassium salt of the 1,5-bis(triisopropylsilyl)pentalene dianion reacted with $ThCl_4$ under salt elimination reaction to afford the bis(η^8-pentalene)thorium complex. The compound was characterized by UV–vis, ^{1}H-, ^{13}C-, ^{29}Si-NMR, and the crystal structure was determined by X-ray diffraction (Scheme 42).

The yield of the deep orange crystals was 70%. The crystals contain a mixture of staggered and eclipsed isomers. The two isomers differ in the relative orientation of the pentalene rings facing the thorium and in the twist angles (defined by the angles between the two bridgehead C–C vectors) of the two pentalene rings. The latter were 83 and 38°. The silicon atoms are 17° bent out of the planes of the five-membered rings away from the metal centre.

The thorium–ring carbon distances ranged from 2.543(10) Å for the bridgehead carbon C2 to 2.908(11) Å for the 'wingtip' carbon C4. The pentalene ring C–C bond lengths ranged from 1.36(2) (C3–C4) to 1.49(2) Å (C2–C3) (Fig. 18, Fig. 19).

Gourier and Caurant [31] investigated the electronic ground state of organouranium(V) compounds influenced by different ligands by electron paramagnetic resonance (EPR). It was shown that the interactions of 5f orbitals with η^8-C_8H_8, η^5-C_5H_5, η^5-C_5Me_5, THF and NR_2 ligands are sufficiently small to conserve the ground state quantum number $J = 5/2$ of the free U(V) ion as a good quantum number for the complex, that the contribution of 5f orbitals to the electronic structure of these compounds is non-bonding, and the metal ligand bonding should involve mainly uranium 6d orbitals.

3.3. Organoactinide catalysis

Evans et al. [12] tested the catalytic activity of $U(C_5Me_5)_3$ in ethylene polymerization. It was found that this uranium complex initiates the polymerization and afforded a polymer with a high molecular mass.

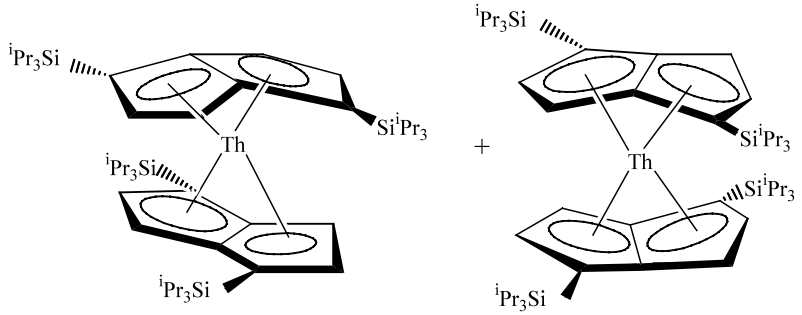

Scheme 42. Synthesis of bis(η^8-pentalene)thorium complex.

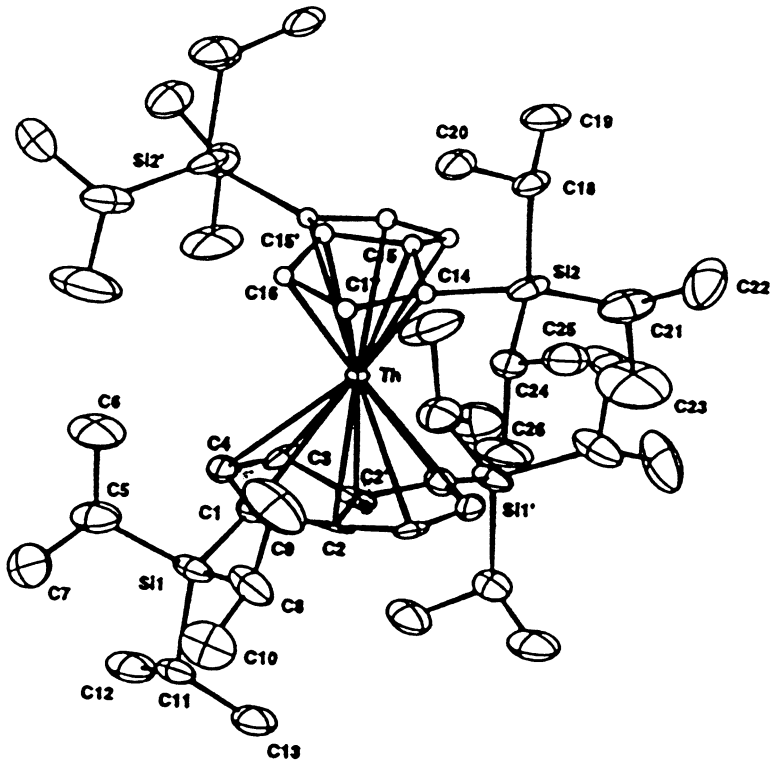

Fig. 18. ORTEP view of the molecular structure of [Th(η^8-C_8H_4{Si^{i}Pr$_3$-1,5}$_2$)$_2$].

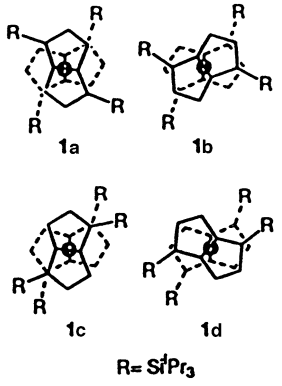

Fig. 19. Isomers of [Th(η^8-C_8H_4{Si^{i}Pr$_3$-1,5}$_2$)$_2$].

Acknowledgements

Financial support of our own work by the Deutsche Forschungsgemeinschaft, the Fonds der Chemischen Industrie and the Otto-von-Guericke-Universität Magdeburg is gratefully acknowledged.

References

[1] (a) C. Alcaraz, U. Groth, Angew. Chem. 109 (1997) 2590;
(b) C. Alcaraz, U. Groth, Angew. Chem. Int. Ed. Engl. 36 (1997) 2480.
[2] Z. Hou, Y. Zhang, T. Yoshimura, Y. Wakatsuki, Organometallics 16 (1997) 2963.
[3] C.P. Casey, S.L. Hallenbeck, J.M. Wright, C.R. Landis, J. Am. Chem. Soc. 119 (1997) 9680.
[4] Z. Xie, Z. Liu, F. Xue, Z. Zhang, T.C.W. Mak, J. Organomet. Chem. 542 (1997) 285.
[5] A.Z. Voskoboynikov, I.N. Parhina, A.K. Schestakova, K.P. Butin, I.P. Beletskaya, L.G. Kuz'mina, J.A.K. Howard, Organometallics 16 (1997) 4041.
[6] D. Baudry, A. Dormond, B. Lachlot, M. Visseaux, G. Zucchi, J. Organomet. Chem. 547 (1997) 157.
[7] L. Mao, Q. Shen, M. Xue, Organometallics 16 (1997) 3711.
[8] K.C. Hultzsch, T.P. Spaniol, J. Okuda, Organometallics 16 (1997) 4845.
[9] Q. Liu, M. Ding, Y. Lin, Y. Xing, J. Organomet. Chem. 548 (1997) 139.
[10] P.W. Roesky, U. Denniger, C.L. Stern, T.J. Marks, Organometallics 16 (1997) 4486.
[11] P.W. Roesky, C.L. Stern, T.J. Marks, Organometallics 16 (1997) 4705.
[12] (a) W.J. Evans, K.J. Forrestal, J.W. Ziller, Angew. Chem. 109 (1997) 798;
(b) W.J. Evans, K.J. Forrestal, J.W. Ziller, Angew. Chem. Int. Ed. Engl. 36 (1997) 798.
[13] P.S. Tanner, J.S. Overby, M.M. Henein, T.P. Hanusa, Chem. Ber./Recueil 130 (1997) 155.
[14] S. Jank, H. Reddmann, H.D. Amberger, J. Alloys Compd. 250 (1997) 387.
[15] Z. Xie, K. Chui, Z. Liu, F. Xue, Z. Zhang, Th.C.W. Mak, J. Sun, J. Organomet. Chem. 549 (1997) 239.
[16] P. Poremba, F.T. Edelmann, Polyhedron 16 (1997) 2067.
[17] Q. Shen, M. Qi, S. Song, L. Zhang, Y. Lin, J. Organomet. Chem. 549 (1997) 95.
[18] W.W. Ma, Z.Z. Wu, R.F. Cai, Z.E. Huang, J. Sun, Polyhedron 16 (1997) 3723.
[19] J. Guan, Q. Shen, R.D. Fischer, J. Organomet. Chem. 549 (1997) 203.

[20] B. Utrecht, S. Jank, H. Reddmann, H.D. Amberger, F.T. Edelmann, N.M. Edelstein, J. Alloys Compd. 250 (1997) 383.
[21] Z. Xie, Z. Liu, K.Y. Chiu, F. Xue, T.H.C.W. Mak, Organometallics 16 (1997) 2460.
[22] D. Tashiro, Y. Kawasaki, S. Sakaguchi, Y. Ishii, J. Org. Chem. 62 (1997) 8141.
[23] W.J. Evans, M.A. Ansari, J.D. Feldman, R.J. Doedens, J.W. Ziller, J. Organomet. Chem. 545–546 (1997) 157.
[24] L.S. Boffa, B.M. Novak, Macromolecules 30 (1997) 3494.
[25] G.A. Molander, W.H. Retsch, J. Am. Chem. Soc. 119 (1997) 8817.
[26] Y. Obora, T. Ohta, C.L. Stern, T.J. Marks, J. Am. Chem. Soc. 119 (1997) 3745.
[27] D. Rabinovich, G.L. Schimke, W.T. Pennigton, J.B. Nielsen, K.D. Abney, Acta Crystallogr. Sect. C 53 (1997) 1794.
[28] D. Rabinovich, R.M. Chamberlin, B.L. Scott, J.B. Nielsen, K.D. Abney, Inorg. Chem. 36 (1997) 4216.
[29] C. Boisson, J.C. Berthet, M. Lance, M. Nierlich, M. Ephritikhine, J. Organomet. Chem. 548 (1997) 9.
[30] F.G.N. Cloke, P.B. Hitchcock, J. Am. Chem. Soc. 119 (1997) 7899.
[31] D. Gourier, D. Caurant, Inorg. Chem. 36 (1997) 5931.